Staurosporine, a Kinase Inhibitor with Antifungal Potential

Evelyne J. Côté

Department of Microbiology and Immunology

McGill University

August 2024

A thesis submitted to McGill University in partial fulfilment of the requirements of the degree of the Masters of Science

Table of Contents

Abstract

In the search for new antifungal agents, one approach is to mine the biodiversity of poorly characterized microbial ecosystems such as the Arctic. We found that an organic extract of the culture supernatant of a novel arctic *Streptomyces species*, *Streptomyces A28*, exhibited broad-spectrum antifungal activity. We hypothesized the active agent in this extract could be an effective antifungal against human fungal pathogens and set out to identify the active agent, characterize its therapeutic index, and probe its mechanism of action. Identification of the active agent as staurosporine (STS) was achieved using liquid chromatography and mass spectrometry. The antifungal activity of STS against a range of fungi was determined by broth microdilution assays, and the cytotoxicity of the compound was evaluated against the human A549 cell line. Overall, STS was found to be a broad-range antifungal *in vitro*. When the antifungal efficacy of STS *in vivo* was evaluated in a mouse model of invasive pulmonary aspergillosis, it was found to be significantly protective. To understand the mechanism of action of STS, we performed phosphoproteomic analysis and cell wall sugar quantification on STS-exposed *A. fumigatus*. We found STS exposure impacted the phosphorylation states of several cell wall sugar synthases and proteins within the cell wall integrity pathway. One of the down-phosphorylated proteins was the β-(1,3)-D-glucan synthase Fks1, and we found a corresponding decrease in β-(1,3)-D-glucan within the STS-exposed *A. fumigatus* cell wall. Based on these results, we tested for synergy between STS and existing antifungals with checkerboard assays and *in vivo*. We discovered the *in vitro* synergy between STS and echinocandins against *A. fumigatus*, although this synergy could not be confirmed *in vivo*. This project shows that identified natural products can bring possibilities and new directions of research for antifungal development through verification of their antifungal activity and investigations into their mechanisms of action.

Résumé

Dans la recherche de nouveaux agents antifongiques, une approche consiste à exploiter la biodiversité d'écosystèmes microbiens mal caractérisés tels que l'Arctique. Nous avons découvert qu'un extrait organique du surnageant de culture d'une nouvelle espèce arctique de *Streptomyces*, *Streptomyces A28*, présentait une activité antifongique à large spectre. Nous avons émis l'hypothèse que l'agent actif de cet extrait pourrait être un antifongique efficace contre les pathogènes fongiques humains, et nous avons entrepris d'identifier l'agent actif, de caractériser son index thérapeutique et d'étudier son mécanisme d'action. La chromatographie liquide et la spectrométrie de masse ont permis d'identifier l'agent actif comme étant la staurosporine (STS). L'activité antifongique de la STS contre une série de champignons a été déterminée par des essais de microdilution en bouillon, et la cytotoxicité du composé a été évaluée contre la lignée cellulaire humaine A549. Dans l'ensemble, le STS s'est révélé être un antifongique à large spectre *in vitro.* Lorsque l'efficacité antifongique du STS a été évaluée in vivo dans un modèle murin d'aspergillose pulmonaire invasive, elle s'est avérée significativement protectrice. Pour comprendre le mécanisme d'action du STS, nous avons effectué une analyse phosphoprotéomique et une quantification des sucres de la paroi cellulaire sur *A. fumigatus* traité au STS. Nous avons constaté que le traitement au STS avait un impact sur les états de phosphorylation de plusieurs synthases de sucres de la paroi cellulaire et de protéines de la voie d'intégrité de la paroi cellulaire. L'une des protéines phosphorylées à la baisse était la β-(1,3)-D-glucan synthase Fks1, et nous avons constaté une diminution correspondante du β-(1,3)-D-glucan dans la paroi cellulaire *d'A. fumigatus* traitée au STS. Sur la base de ces résultats, nous avons recherché une synergie entre le STS et les antifongiques existants au moyen d'essais en damier et in vivo. Nous avons découvert une synergie *in vitro* entre les STS et les échinocandines contre A. fumigatus, bien que cette synergie n'ait pas

pu être confirmée *in vivo*. Ce projet montre que les produits naturels identifiés peuvent offrir des possibilités et de nouvelles directions de recherche pour le développement d'antifongiques grâce à la vérification de leur activité antifongique et à l'étude de leurs mécanismes d'action.

Acknowledgments

I would like to thank my thesis supervisor Dr. Don Sheppard for all the counseling, connections, knowledge, and training to become a mycologist he has provided. My gratitude also extends to my co-supervisor, Dr. Lyle Whyte, for accepting me as an Honour's student in 2021 and providing the first step to starting this journey. I could not have asked for a better start in my choice of career, and for all the support I received to go on to the next step.

I could not have completed this project without the members of the Sheppard lab. My first thanks must go to Dr. François Le Mauff for training me in my first year at the Sheppard lab, thus providing me with a strong foundation in research. I also thank Dr. Thi Tuyet Mai Nguyen for performing the animal experiments, a critical component of this project. To David, Josée, and Ira, thank you for answering all my questions and the sanity checks.

I want to extend my gratitude and appreciation to my committee members, Dr. Dao Nguyen, and Dr. Albert Berghuis. The encouragement and direction provided have been essential for the completion and quality of this project. I would also like to acknowledge the Proteomics and Molecular Analysis, and the Histopathology platforms for their support of this project.

Finally, I want to thank my family, friends, and partner for encouraging me through my time as a graduate student, and for supporting me through the more difficult times these last two years.

Contribution of Authors

The majority of the thesis project was designed, performed, analysed, and written by Evelyne J. Côté, under the co-supervision of Don Sheppard and Lyle Whyte. Adam Classen, Evan Marcolefas, and Jennifer Ronholm provided the initial data demonstrating the antifungal activity of *S. A28* extract against the fungi that cause dairy spoilage. Xuefei Chen and Gerry Wright contributed to the identification of the *S. A28* extract active agent as STS. François Le Mauff contributed to the experiments and data analysis related to the *S. A28* extract. The animal experiments were all performed by Thi Tuyet Mai Nguyen, with contributions from Evelyne J. Côté to the design of the experiments and the data analysis.

List of Figures

List of Tables

List of Abbreviations

DNA – Deoxyribonucleic acid

RNA – Ribonucleic acid

STS – Staurosporine

HIV – Human Immunodeficiency Virus

ROS – Reactive oxygen species

5-FC – 5-fluorocytosine

5-FU – 5-fluorouracil

CWI – Calcofluor white

rRNA – Ribosomal ribonucleic acid

WHO – World Health Organization

YPD – yeast peptone dextrose

PBS – Phosphate buffer saline

PBS-T – Phosphate-buffered saline with Tween-80

w/v – Weight/volume

v/v – Volume/volume

PDB – potato dextrose broth

CO_2 – carbon dioxide

SAB – Sabraroud

ATCC – American Type Culture Collection

RPM – Rotations per minute

MTT – 3-(4,5-dimethylthiazol-2-yl)-2,5-diphenyltetrazolium bromide

TSB – Tryptic soy broth

CLSI - Clinical and laboratory standard institute

RPMI – Roswell Park Memorial Institute

DMSO – Dimethyl sulfoxide

XTT – 2,3-Bis-(2-Methoxy-4-Nitro-5-Sulfophenyl)-2H-Tetrazolium-5-Carboxanilide)

H_2O – Water

ACN – acetonitrile

TFA – trifluoroacetic acid

MS – mass spectrometry

MALDI-TOF – matrix-assisted laser desorption/ionization time-of-flight

GFP – green fluorescent protein

IR-OPO – Infrared optical parametric oscillator

CFW – Calcofluor white

PI – Post-infection

Na_3VO_4 – Sodium orthovanadate

NaPPi – Sodium pyrophosphate

DTT – Dithiothreitol

NP-40 – Nonyl phenoxypolyethoxylethanol

GO – Gene Ontology

dH_2O – Deionized water

NaOH – Sodium hydroxide

$NaBH_4$ – Sodium borohydride

HCl – Hydrochloric acid

ELISA – enzyme-linked immunosorbent assay

HRP – Horseradish peroxidase

H_2SO_4 – Sulfuric acid

TMB – 3,3',5,5'-tetramethylbenzidine

IC_{50} – Half maximal inhibitory concentration

UCN-01 – 7-hydroxystaurosporine

K252a – Methyl (13S,14R,16R)-14-hydroxy-13-methyl-5-oxo-6,7,13,14,15,16-hexahydro-5H-13,16-epoxydiindolo[1,2,3-fg:3′,2′,1′-kl]pyrrolo[3,4-i][1,6]benzodiazocine-14-carboxylate.

GlcNAc – N-acetylglucosamine

LC – Liquid chromatography

MIC – Minimum inhibitory concentration

MEC – Minimum effective concentration

Chapter 1: Introduction and Literature Review

1.1 Overview

Fungal infections affect more than a billion people annually, among which more than 6 million become severely ill with invasive fungal disease, and 3 million people will die (1, 2). The progress of medical innovation has resulted in an increasingly large population of immunocompromised patients who are especially susceptible to invasive fungal infections (3). Despite these dramatic statistics, there has been inadequate investment in research and development of new diagnostic tools or treatments to fight fungal disease (1, 4). As a result, our current antifungal armamentarium consists of only five classes of antifungals which only target three fungal pathways: the pyrimidine analogs target DNA and RNA synthesis, echinocandins target β-(1,3)-D-glucan synthesis and the remaining classes target the fungal membrane sterol ergosterol (5). In addition, rates of resistance to these antifungals are on the rise (1). Collectively, these observations highlight the urgent need to develop new antifungals to preserve human lives (4, 6, 7).

1.2 Fungal infections and their significance

Pathogenic fungi comprise a small minority of species within the fungal kingdom, accounting for only ~300 of the estimated more than 1.5 million fungal species (8). Infections by pathogenic fungi, however, affect over a billion people each year (9). These infections include superficial infections, such as of the hair, skin, and nails, as well as potentially life-threatening invasive fungal disease (9). Superficial fungal infections are the most common, with nearly a billion people affected each year worldwide, but typically are not associated with high morbidity or mortality (10). In comparison, while invasive fungal disease is much less common, the mortality of these

infections can exceed 50% even with available and effective treatments (10). 6.55 million people are estimated to be affected by life-threatening fungal disease each year, and these infections are associated with an estimated 3.75 million deaths per year (2). There are several reasons why these numbers are so high. Firstly, fungal diseases often develop with non-specific symptoms, thus diagnosis is often delayed until the disease is at an advanced stage (11). Secondly, the population most susceptible to invasive fungal diseases are immunocompromised patients with other co-morbidities, further complicating treatment (12). Examples include people with HIV, cancer patients receiving chemotherapy, and organ transplant recipients on immunosuppressants (13).

The prevalence and mortality of invasive fungal diseases are expected to continue to rise for multiple reasons. First, advances in medical therapy continue to result in increased numbers of immunocompromised patients at risk (14, 15). Furthermore, the rise in resistance to all available antifungal classes threatens the efficacy of our currently available tools to reduce mortality (4, 16). Finally, it is theorized that climate change may increase the risk of fungal disease (17). Changes in weather patterns can cause the displacement of fungi from their natural habitat or an expansion of their habitat, causing endemic fungal disease to spread to new areas (18). Higher global temperature increases the occurrence of natural disasters, during which fungal infections are a substantial risk due to contamination of wounds with soil, water, and debris (19). Perhaps most concerningly, a higher global temperature is also hypothesized to place more selective pressure on fungi to increase their thermotolerance. Most fungi are unable to grow at the human body temperature of 37˚C, however, adaptation to growth at higher temperatures could increase the risk of organisms emerging that are capable of causing human disease (17, 20). Fungal diseases have been neglected for decades and are predicted to have an even greater impact on society unless new developments in diagnosis and especially treatment occur.

1.3 *Aspergillus fumigatus*

The genus *Aspergillus* comprises over 200 species, many of which are extremely useful in multiple industries due to their production of useful metabolites (21). Very few *Aspergilli* can cause disease in humans (21). Those species that do can do so as a consequence of secreted toxins, such as aflatoxin, or as the causative agents of infection (21). *Aspergillus fumigatus* is the most common cause of human *Aspergillus* infections (22). It is a saprotrophic fungus that grows in the form of vegetative filamentous cells (mycelia) in decaying organic matter or the soil. It is ubiquitous in the environment and has an essential environmental role in carbon and nitrogen recycling (23, 24). *A. fumigatus* relies on asexual reproduction to spread in its environment, and produce large amounts of conidia that are dispersed in the air (22).

1.3.1 A. fumigatus infection and virulence factors

Traits that allow *A. fumigatus* to thrive in its environment also contribute to its pathogenesis. Due to the large production of conidia to disperse in its environment, the most common route of exposure to *A. fumigatus* is the inhalation of conidia: it is estimated that humans inhale 100-1000 conidia per day, and 37% of lung biopsies from healthy patients were found to contain *Aspergillus* DNA (25, 26). In the normal host, these inhaled conidia are usually cleared by the mucociliary elevator, or phagocytosed and killed by alveolar macrophages (26). A key first line of antimicrobial defence for humans is the body temperature at 37˚C, but in the environment, *A. fumigatus* can grow within decaying organic matter, such as compost, that can exceed this temperature (22). Thus, as the human body temperature is optimal for *A. fumigatus* growth, if the conidia are not cleared by these innate responses, they can germinate within 4-6 hours upon entry into the lungs (26). This

event can trigger an inflammatory response resulting in the recruitment of neutrophils, the most important immune cell type for defence against *Aspergillus*, as they can destroy hyphae (22). If both of these levels of protective response are impaired or absent, the lungs can be colonized or invaded by *A. fumigatus*, leading to chronic or invasive aspergillosis (25, 27).

The *Aspergillus* cell wall is another major factor that contributes to virulence. The cell wall consists largely of polysaccharides, such as β-glucans like β-(1,3)-D-glucan, chitin, α-glucans, mannans, galactomannans, and galactosaminogalactan, with a smaller amount of proteins and pigment molecules that have essential roles in the cell wall (28, 29). During the life cycle of *A. fumigatus*, the content of the cell wall varies: during the conidia stage, hydrophobin proteins and melanin pigment make up the superficial rodlet layer, which has multiple roles: not only is it required for waterproofing and buoyancy in the air, but this layer conceals many of the polysaccharides that have immunostimulatory properties, masking conidia from the immune system (30-32). When germination begins, the rodlet layer is degraded resulting in more glucan exposure during germination, with chitin serving as the skeleton to give the cell wall more rigidity (29). Synthesis of galactosaminogalactan, which is not present in conidia, begins after germination to act as a major adhesin for mycelium (29). In mature hyphae, the cell wall is structured as chitin, α-, and β-glucans forming the core with mannans covalently bound, and galactomannan and galactosaminogalactan as the outermost polysaccharides, cloaking the more immunostimulatory glucans (33). Aside from the life cycle, dynamic changes in cell wall composition also allow for survival under different stresses, from compost to within an infected host (29). Both cell wall polysaccharides and proteins are essential for initial adhesion to host tissues, allowing for hyphal invasion of host tissues and biofilm formation (34). The latter is extremely important for fungal

survival within the human host, as a biofilm protects the hyphae from both the immune response and killing by antifungal drugs (27).

Other virulence factors contribute to the pathogenicity of *A. fumigatus* such as the production of toxins, proteases, and siderophores. The fungus secretes multiple mycotoxins to protect itself against predators and competitors, which extends toward the host's immune system (35). The most potent mycotoxin is gliotoxin, which suppresses macrophage and neutrophil phagocytosis, and impairs ROS production (36, 37) Each mycotoxin has unique effects, but all can inhibit leukocyte function (38). Proteases and siderophores are essential for fungal pathogen survival: proteases are used by *A. fumigatus* to disorganize the actin cytoskeleton in the alveolar epithelial cells and destroy their focal adhesions, allowing for fungal invasion (39) In the host, the innate immune system sequesters iron to defend against invading microorganisms, but *A. fumigatus* utilizes extracellular siderophores to acquire iron, neutralizing this defence, and promote hyphal growth (40).

1.3.2 Diseases caused by A. fumigatus exposure and infection.

Diseases following exposure to *A. fumigatus* conidia depend on the pulmonary and immunologic health of the host. In immunocompetent hosts with normal lung function, there is little to no risk of fungal disease upon exposure but a subset of this population can be predisposed to atopy, in which conidia can act as allergens to cause severe asthma with fungal hypersensitization (25).

Impairment of lung function, however, allows the conidia to remain in the lung to germinate within the airways (41). When hyphae grow within the airways of hosts that are not significantly immunocompromised, there is a range of possible outcomes (25, 41). Allergic bronchopulmonary

aspergillosis can develop in response to the continuous hyphal antigens, a severe allergic reaction to the fungal antigens that can lead to severe asthma and bronchiectasis (23). The estimated global prevalence of this disease is estimated to be approximately 4.8 million cases (42). If the hyphae grow within pre-existing cavities of the lungs, such as those associated with pulmonary tuberculosis, balls of fungi called aspergillomas can form leading to chronic inflammation and haemoptysis (22, 27, 43). Chronic bronchitis is also a possible outcome of *Aspergillus* colonization and is associated with neutrophilic inflammation. If aspergillosis or aspergillus bronchitis remains untreated, these outcomes can further develop into a chronic microinvasive infection of the lung with inflammation termed chronic pulmonary aspergillosis (25). The most recent estimated incidence of chronic pulmonary aspergillosis is over 1.8 million cases per year, nearly 20% of which will lead to death (2).

In contrast, if the human host is immunocompromised, either from innate immune defects, chemotherapy, or other immunosuppressive therapies, infection by *A. fumigatus* can result in acute invasive aspergillosis (25). This disease occurs when viable hyphae rapidly invade the pulmonary tissue causing necrosis and thrombosis (27). *A. fumigatus* can even spread beyond the respiratory system via the bloodstream to the liver, spleen, or central nervous system (25). Invasive aspergillosis currently has a crude annual mortality burden of 2.12 million cases per year (2). Invasive aspergillosis is associated with a mortality rate of 40%, which can increase if there is resistance to antifungals (4). The high incidence and mortality of invasive aspergillosis are in part due to delays in initiating therapy due to the lack of sensitive and specific non-invasive tests for these conditions (25, 44, 45).

1.3.3 Antifungal therapies

The first family of antifungals to be used in the treatment of *Aspergillus* infections were pyrimidine analogues such as 5-fluorocytosine (5-FC). These agents, developed in the 1950s, are not directed at a unique fungal target (46). Antifungal specificity relies on the fact that 5-FC is a prodrug that is taken up by cytosine permease within the fungal cell membrane and metabolized by fungal cytosine deaminase to 5-fluorouracil (5-FU) (46). 5-FU can be further processed to become 5-fluorouridine monophosphate or 5-fluorouridine, which can be incorporated into DNA and RNA and interfere with their synthesis (47, 48). Mammalian cells do not readily take up 5-FC and lack cytosine deaminase and only fungi with cytosine deaminase are susceptible to 5-FC (47, 49). Even though *A. fumigatus* does have cytosine deaminase, 5-FC has limited effectiveness under physiological conditions and resistance occurs rapidly upon exposure to this agent as a monotherapy (50). 5-FC is not commonly used clinically to treat *Aspergillus*-induced disease (51).

The four other approved classes of antifungal drugs target two macromolecules unique to fungi: the membrane lipid ergosterol and the cell wall polysaccharide β-(1,3)-D-glucan (52). In contrast to human cells, fungal cell membranes rely on ergosterol rather than cholesterol for membrane fluidity, and this difference is exploited by three antifungal classes, the azoles, the polyenes, and the allylamines, (16, 25). Azoles inhibit the 14-α sterol demethylase A Cyp51, which mediates the demethylation of lanosterol, another intermediate molecule in the ergosterol synthesis pathway (25, 53). The inhibition of Cyp51 depletes the ergosterol from the cell membrane and leads to the accumulation of toxic sterol intermediates, resulting in fungal growth arrest (25, 53). Triazoles such as voriconazole, itraconazole, and posaconazole are the first-line drugs for aspergillosis, as they are well tolerated and are available in oral form (54, 55).

Polyenes, such as amphotericin B, directly target ergosterol by irreversibly binding to it and forming pores within the fungal plasma membrane, leading to cellular leakage and cell death (25, 56). Amphotericin B, the most commonly used polyene for the treatment of invasive fungal diseases, has recently been found to have a second mechanism of action of drawing ergosterol out of the fungal plasma membrane, acting as an extramembranous sponge (57, 58). Polyenes are effective against a broad range of fungal pathogens and can exert fungistatic or fungicidal activity depending on the dose, pH, and targeted fungal pathogen (55). As non-specific binding of polyenes to mammalian cholesterol can occur, the clinical use of amphotericin B is limited by observed renal and other cellular toxicities (59). Newer formulations such as the use of liposomes containing amphotericin B have been shown to reduce this toxicity (59). Amphotericin B is an alternative first-line treatment to azoles for aspergillosis, and it is most commonly used for drug-resistant infections (54).

Allylamines, of which only terbinafine is in clinical use, cause an accumulation of an intermediate in the ergosterol synthesis pathway called squalene by targeting the squalene epoxidase (60). Terbinafine is mainly used to treat superficial fungal infections and has limited activity against invasive fungal diseases such as invasive aspergillosis (16, 61).

The most recent class of approved antifungals, the echinocandins, interfere with the synthesis of β-(1,3)-D-glucan through the inhibition of Fks1 (25, 62). Lack of β-(1,3)-D-glucan in the cell wall leads to osmotic instability of the fungal cell (63). Echinocandins exhibit an impressive safety profile due to the specificity of their target, but unfortunately can only be administered intravenously (64). Echinocandin activity is dependent on the fungal pathogen. They exhibit fungicidal activity against *Candida* and are therefore the first-line drugs for invasive candidiasis (63). Against *Aspergillus*, however, echinocandins are fungistatic. Treatment with

echinocandins causes lysis of hyphal tips but the subapical compartments of the hyphae remain viable (65). This intrinsic reduced susceptibility is reliant on molecular mechanisms such as the cell wall integrity (CWI) pathway described below (66). Echinocandins are used as a salvage therapy for refractory or intolerant invasive aspergillosis cases (67).

Combination therapy, or the use of more than one antifungal to treat a fungal infection, has proven an effective strategy for some fungi; 5-FC with amphotericin B to treat cryptococcosis and posaconazole with amphotericin B to treat mucormycosis (47, 68). However combination therapies can be complex, the drugs chosen may be synergistic or antagonistic, depending on the concentrations used, and some combinations can increase the toxicity of treatment (68).

1.3.4 Antifungal resistance and its impact

Antifungal resistance directly impacts the treatment of fungal disease and can be intrinsic or acquired. Fungi can be intrinsically resistant to antifungals due to a variety of mechanisms including biofilm formation, in which the extracellular matrix physically protects the hyphae, or due to a lack of the antifungal target molecule, as exemplified by the resistance to echinocandins by fungal genera *Mucor* and *Cryptococcus* due to the limited or absent β-(1,3)-D-glucan in their cell walls (69, 70). Cellular stress responses also play important roles in intrinsic resistance, such as the CWI pathway observed in many fungi, including *A. fumigatus*. This pathway is a compensatory mechanism triggered by the depletion of β-(1,3)-D-glucan in the cell wall after echinocandin treatment (71). The resulting cell wall stress is detected by a mechanosensor called Wsc1, which activates a cascade of kinases including protein kinase C (71). Several transcription factors are activated, such as RlmA, which upregulate the transcription of cell wall polymer synthase genes including: ß-(1,3)-D-glucan synthase *fks1*, α-glucan synthase *ags1*, and three chitin

synthases *chsE*, *chsF,* and *chsG* (72). One of the downstream effects of CWI pathway activation is an increased chitin content in the cell wall, which can compensate for the loss of β-(1,3)-D-glucan and increase echinocandin resistance to *A. fumigatus* (65, 73). Intrinsic resistance against specific drugs within a class of antifungals has also been observed. *A. fumigatus* is intrinsically resistant to fluconazole, despite being susceptible to other members of the azole class, which is hypothesized to be because of a naturally occurring amino acid substitution of Cyp51A, the *Aspergillus* Cyp51 enzyme (69, 74).

Acquired resistance has been observed in pathogenic fungi against all approved antifungal classes; mechanisms can range from induction of efflux mechanisms to overexpression or mutation of the target (47, 75, 76). Two major mechanisms of acquired resistance in fungi against azoles are drug efflux pumps, upregulating plasma membrane pumps to reduce intracellular drug concentration, and the overexpression of the Cyp51 enzyme (77-79). Alteration of the target, however, has been observed as adaptative resistance against azoles, polyenes, and echinocandins (78). For azole resistance, alterations in the *cyp51* gene result in amino acid substitutions in the enzyme that reduce azole susceptibility (80-82). Genomic sequencing of clinical polyene-resistant fungal strains has shown mutations in a range of ergosterol synthesis genes, which lead to the accumulation of different sterols in the fungal membrane (83). Reduced susceptibility to echinocandins has been observed with point mutations in hot spot regions of Fks1. These mutations are much more commonly observed in *Candida* but some clinical cases of *A. fumigatus* with Fks1 mutations have been reported (84-88).

The overuse of one class of antifungals can accelerate the development of resistance leading to increased dependence on other classes (89). For example, the widespread clinical and agricultural use of azoles has led to a dramatic increase in antifungal resistance (76). The increased

observed azole resistance, as well as the limitations on toxicity and drug interactions with polyenes, has led to increased use of echinocandins for these infections (89, 90). Although *in vivo* resistance of *A. fumigatus* against echinocandins is uncommon, there have been increasing reports of clinical cases of aspergillosis patients failing echinocandin treatments (84, 91). The increased reliance on this class due to azole resistance increases the risk of emerging echinocandin-resistant aspergillosis (92).

Acquired resistance is a major challenge in the clinic as it can dramatically increase mortality rates. For example, if *A. fumigatus* acquires resistance to amphotericin B or azoles, the mortality rate of invasive aspergillosis jumps to as high as 90% (4). Despite such impact, antifungal resistance has been traditionally excluded from antimicrobial resistance and stewardship programs, with systemic inaction against the crisis (3, 93). Fortunately, it has gained recent worldwide attention: in 2022, the World Health Organization (WHO) released a fungal priority pathogens list describing the most significant pathogens, and what research and interventions are needed in response (94). *A. fumigatus* was classed under "critical," the highest priority group, emphasizing its threat to society (94).

1.4 Discovery of new antifungal therapies

1.4.1 Limitations on antifungal development

As clinicians are faced with a shrinking arsenal of antifungals to treat invasive fungal disease due to the rising resistance rates, there is an urgent need for novel and broad-spectrum antifungals. The antimicrobial discovery pipeline, however, contains very few antifungal candidates as most pharmaceutical companies are not invested in the development of antifungals (4). Antifungal development has many challenges, the most important of which is the identification of fungal-

specific metabolic targets, as fungi are eukaryotic organisms that share many of their biological processes with human cells (95). Many of the currently exploited targets share a close enough relationship with human analogues that host toxicity can be limiting (95). For example, polyenes only exhibit partial selectivity for ergosterol over cholesterol, and can therefore exhibit toxic effects on human cells (96). It has been suggested toxicity can be attributed to the extraction of cholesterol from the plasma membrane of host cells by amphotericin B to create extramembranous sponges (57). Furthermore, identification of truly essential targets has proven challenging as fungi can have intrinsic compensatory pathways to bypass the antifungal effects of new agents (97). One example, described above, is the CWI pathway that allows the fungi to survive previously effective concentrations of echinocandins (65, 98). Off-target effects are also a major concern with antifungals, which is exemplified by 5-FC (99). The selectivity of 5-FC is based on the presence of cytosine deaminase in fungi but not in mammalian cells, yet it has been discovered that 5-FC can be converted to 5-FU in humans by the intestinal microflora, contributing to the toxicity of this drug (47, 49).

1.4.2 Methods of antimicrobial discovery

Generally speaking, novel antimicrobials have either been generated through screening of molecules created through synthetic chemistry, or sourced from natural products (100). Synthetic chemistry has been associated with several successes in the antifungal space, with the development of olorofim as one of the best examples (101). Olorofim is the first representative of a new class of chemically synthesized antifungal drugs called orotomides, recently developed by F2G Limited, with a novel drug target (102). Orotomides inhibit dihydroorotate dehydrogenase, an enzyme that catalyzes the fourth step of the pyrimidine de novo synthesis pathway, leading to cell lysis (101).

Preclinical studies have demonstrated the activity of olorofim against pathogens such as *A. fumigatus* both *in vitro* and *in vivo*, and it is currently in phase 3 clinical trials (102). Medicinal chemistry has also been used to modify antifungal natural products with increased activity, more flexible administration, and limiting the rate of resistance (103). One example is the development of ibrexafungerp, a new echinocandin that can be administered orally (104). It has a similar mechanism to first-generation echinocandins, but with a different chemical structure and exhibits only a partial overlap of the binding sites, thereby thus limiting cross-resistance and the rate of resistance (105).

Despite this recent success, the majority of antimicrobial discovery work has relied on the identification of secondary metabolites with antimicrobial activity that are produced by microorganisms from diverse natural environments (106). Indeed, 70% of all antimicrobials in current use are derived from this process (107). Antifungals are not the exception, as amphotericin B and echinocandin B, the first drug of the echinocandin drug class, were originally discovered as natural products (108, 109). Natural product screening, however, frequently reisolates previously characterized molecules, and the inefficiency of this process serves as another reason for the withdrawal of pharmaceutical companies from antimicrobial development (110). To improve the efficacy of this method, researchers are now seeking to bioprospect poorly characterized microbiomes, either animal or environmental, in the hope that they may host novel bioactive molecules (111). One recent example of success using this new approach was demonstrated by the isolation of a promising antifungal molecule called turbinmicin from the microbiome of the *Micromonospora* sea squirt species (112). Turbinmicin is a member of the type II highly oxidized polyketides, it was found to have both *in vitro* and *in vivo* antifungal activity against several multi-drug resistant pathogens including *Candida auris* and *A. fumigatus* (112). Turbinmicin mediates

antifungal activity by impairing vesicle trafficking, a unique mechanism of action not previously described (112, 113). Other unique microbiomes currently under investigation include the Arctic, which has been found to harbour novel biosynthetic gene clusters and secondary metabolites (114, 115).

1.5 Isolation and preliminary characterization of a *Streptomyces* species (*S. A28*) whose secretome exhibits antifungal properties

An expedition led by Dr. Lyle Whyte's lab at McGill Arctic Research Station on Axel Heiberg Island, Nunavut, Canada collected Arctic bacterial isolates from a range of soil samples (115). The antifungal potential of these Artic isolates were assessed against fungi that cause dairy spoilage (116). The isolates were first co-cultured on agar with fungi isolated from yogurt such as *Penicillium roqueforti* (116). From this assay, one isolate, A28, inhibited fungal growth in co-culture (116). Organic extracts of A28 culture supernatants exhibited a similar profile of antifungal activity against dairy fungal pathogens, suggesting that this organism secreted substances with antifungal activity (116). Whole genome sequencing revealed this strain to be a novel species of the genus *Streptomyces*, with the closest relative being *Streptomyces camponoticapitis* based on 16S rRNA sequencing (98.02% similarity) (116). This isolate was named *S. A28*, and genome analysis for predicted biosynthetic gene cluster was performed by antiSMASH, a software to mine microbial genomes (117). A preliminary analysis of the *S. A28* genome revealed a variety of biosynthetic gene clusters with the potential to encode novel antimicrobial compounds including non-ribosomal peptide synthetases, aryl polyenes, terpenes, and polyketide synthase types I, II, and III (116).

1.6 Research hypothesis

Given the activity of organic extracts of *S. A28* culture supernatant against dairy fungi, we hypothesized that molecule(s) produced by *S. A28* could also exhibit antifungal activity against human fungal pathogens.

1.7 Research objectives

1. Identify the compound(s) exhibiting antifungal activity within *S. A28* organic extract.
2. Characterize the antifungal activity and mammalian tolerability of the active agent, alone and in combination with existing antifungals.
3. Identify the active agent's mechanism of action.

Preface to Chapter 2

The screening of natural products in poorly characterized environments, such as the Arctic, has been hypothesized to yield novel antimicrobials. An organic extract of culture supernatants from the Arctic bacteria *S. A28* demonstrated antifungal activity against the fungi that cause dairy spoilage. In this chapter, the activity of the organic extract against human fungal pathogens was evaluated. The active agent of the extract, STS, was identified and evaluated for antifungal activity and tolerability *in vitro*, and in an animal model of invasive aspergillosis. The antifungal mechanism of action of STS was investigated *in vitro*, and STS synergy with existing antifungals was evaluated both *in vitro* and *in vivo*.

Chapter 2: Staurosporine, a kinase inhibitor with antifungal potential

Evelyne Jane Côté[1,2], Adam Classen[3#], Evan Marcolefas[4], Jennifer Ronholm[3], Lyle Whyte[4], Xuefei Chen[5], Gerard Wright[5], Thi Tuyet Mai Nguyen[2], Donald C. Sheppard[1,2], François Le Mauff[2]

[1]Department of Microbiology and Immunology, McGill University, Montreal, Canada. [2]Infectious Diseases and Immunity in Global Health Program, Research Institute of the McGill University Health Center, Montreal, Canada. [3]Department of Food Science and Agricultural Chemistry, McGill University, Montreal, Canada. [4]Department of Natural Resources Sciences, McGill University, Montreal, Canada. [5]Department of Biochemistry and Biomedical Sciences, McMaster University, Hamilton, Canada. #Current address: Department of Experimental Therapeutics, BC Cancer, Vancouver, Canada.

Abstract:

Introduction: In the search for new antifungal agents, one approach is to mine the biodiversity of poorly characterized microbial ecosystems such as the Arctic. We previously reported that an organic extract of the culture supernatant of a novel arctic *Streptomyces*, *Streptomyces A28*, had antifungal activity against dairy spoilage fungal pathogens. We hypothesized that this activity could extend to human fungal pathogens, and sought to identify the active agent and evaluate its therapeutic potential.

Methods: Identification of the active agent was achieved using liquid chromatography and mass spectrometry. Antifungal susceptibility assays were performed using micro-broth dilution protocol, and cytotoxicity was evaluated against the human A549 cell line. Synergy with existing antifungals was investigated with checkerboard assays. Preliminary investigations into the mechanism of action of the active agent were performed using phosphoproteomic analysis and cell wall sugar quantification. Antifungal drug efficacy was evaluated in a mouse model of invasive pulmonary aspergillosis.

Results: The antifungal activity of the *S. A28* culture supernatant extract was determined to be mediated by the previously described broad-spectrum kinase inhibitor staurosporine (STS). STS, and some of its derivatives, were found to exhibit potent antifungal fungal activity against *Aspergillus fumigatus in vitro*. We found that 0.4 mg/kg of STS was well tolerated in mice and was significantly protective against invasive aspergillosis. *A. fumigatus* exposed to STS had significant changes in the phosphorylation states of several cell wall sugar synthases and cell wall integrity (CWI) pathway proteins, including a down-phosphorylation of the Fks1 enzyme. Consistent with

this observation, cell wall analysis confirmed that STS exposure resulted in a reduction of β-(1,3)-D-glucan content in the cell wall, and STS demonstrated antifungal synergy with the Fks1 inhibitor caspofungin against *A. fumigatus in vitro*. However, this phenomenon was not observed *in vivo* in a mouse model of invasive aspergillosis.

Conclusions: STS was found to exhibit antifungal activity against *A. fumigatus in vitro* and act as a well-tolerated antifungal therapy *in vivo*. Preliminary studies of the mechanism of action of STS suggested that down-regulation of β-(1,3)-D-glucan could contribute to the antifungal activity of this agent and synergy of STS with echinocandins was observed *in vitro* but not *in vivo.* These studies have the potential to advance the development of an urgently needed solution to preserve and improve the efficacy of echinocandins against invasive aspergillosis.

Introduction

Humans are exposed to fungi every day through the inhalation of *Aspergillus* conidia (118). In immunocompetent people with normal lung function, these conidia are eliminated (25). Immunocompromised people can fail at eliminating these conidia, which can then germinate into hyphae to invade the surrounding tissue (27). This becomes a necrotizing pneumonia called invasive aspergillosis, of which *Aspergillus fumigatus* is the most common causative agent. It has the highest estimated crude annual mortality among invasive fungal diseases at 2.12 million (2). The susceptible population to invasive aspergillosis is typically immunocompromised patients with other co-morbidities, further complicating treatment (12). Triazoles such as voriconazole and itraconazole are the first-line drugs for aspergillosis, but their widespread clinical and agricultural use has led to a dramatic increase in antifungal resistance (54, 55, 76). As the arsenal of antifungals to treat invasive aspergillosis, and invasive fungal disease in general, is shrinking due to the rising resistance rates, there is an urgent need for novel and broad-spectrum antifungals (4).

Novel antimicrobials have commonly been discovered through the screening of natural products produced by environmental microorganisms (100). Screening microbial secondary metabolites for antimicrobial activity, however, frequently reisolates previously characterized molecules, contributing to the withdrawal of pharmaceutical companies from antimicrobial development (110). To improve the efficacy of this method, some researchers have turned to bioprospecting poorly characterized microbiomes, either animal or environmental, in an effort to increase the likelihood of novel bioactive molecule discovery (111). One such microbiome currently under investigation is the Arctic, which has been reported to harbour organisms containing novel biosynthetic gene clusters and secondary metabolites (114, 115).

In 2019, an expedition led by Dr. Lyle Whyte's lab at McGill Arctic Research Station on Axel Heiberg Island, Nunavut, Canada collected Arctic bacterial isolates from a range of soil samples (115). These isolates were screened for antifungal activity against fungi that cause dairy spoilage (116). An organic extract of culture supernatants from one novel *Streptomyces* species (*A28*), exhibited antifungal activity against fungi that cause dairy spoilage (116). Genomic analysis of *S. A28* revealed a variety of biosynthetic gene clusters with the potential to encode novel antimicrobial compounds: non-ribosomal peptide synthetases, aryl polyenes, terpenes, and polyketide synthase types I, II, and III (116). The observed antifungal activity combined with the biosynthetic gene cluster analysis suggested that *S. A28* may secrete one or more novel antifungal compounds. We hypothesized that molecule(s) present in the organic extract of *S. A28* culture supernatant could also exhibit antifungal activity against human fungal pathogens.

Methods and Materials

Fungal strains

A. fumigatus conidia from the wild-type strain Af293 were collected from colonies grown on plates with yeast extract-peptone-dextrose or YPD (BD Difco™) and 1.5% agar (VWR) incubated for 3 days at 37°C for *in vitro* assays, and 6 days for *in vivo* experiments. Conidia were harvested by washing the plate with phosphate-buffered saline (BioShop) with 0.1% w/v of Tween-80 (BioShop) or PBS-T. *Rhizopus oryzae* conidia were collected from colonies grown on potato-dextrose broth or PDB (BD Difco™) agar at 37˚C, in 5% CO_2 for 3 days. Hyphal fragments were removed by filtration with a 40µm cell strainer. *Candida albicans* SC5314, *Candida glabrata*, *Candida tropicalis*, *Candida parapsilosis*, *Candida krusei*, *Candida auris* (ATCC), and *Cryptococcus neoformans* were maintained on Sabouraud (BD Difco™) agar and precultured in YPD broth overnight at 30˚C and 200 rpm before the relevant assays.

Cell cultures and assays

The A549 lung epithelial cell line (ATCC) was maintained in F12K medium (Kaigh's modification) with heat-inactivated fetal bovine serum and 1% penicillin and streptomycin (all from Wisent, Inc.), incubated at 37˚C 5% CO_2 with passages occurring every 3-4 days depending on confluency, never exceeding 80% confluency. For cytotoxicity assays, a final concentration of 10,000 cells/well was dispensed into a cell-treated 96-well plate with a round bottom (Grenier Bio-one). These cells were incubated for 24 hours at 37˚C 5% CO_2, followed by another 24-hour incubation under experimental conditions. The MTT assay was used to measure the viability of the cells: 10 µL of a 5 mg/mL 3-(4,5-dimethylthiazol-2-yl)-2,5-diphenyltetrazolium bromide (MTT) in PBS was dispensed into each well. After an incubation of 4 hours at 37˚C 5% CO_2, the

supernatant was aspirated and 50 µL of DMSO was dispensed to dissolve the resulting precipitate. The absorbance at 540nm was measured with a spectrophotometer (Infinite M200, Tecan) (119).

S. A28 culture and organic extraction of culture supernatant

S. A28 bacteria were streaked on tryptone soy broth or TSB agar (BD Difco™) and incubated at 25˚C for three days. A seedling culture was then started using a single colony of *S. A28* dispersed in 20 mL of liquid TSB (BD Difco™) and then incubated at 25˚C, 250 rpm for seven days. This culture was filtered out through a 70 µm cell strainer, and 1% v/v filtrate was used to inoculate 200 mL of TSB. The culture was incubated at 17˚C at 250 rpm for 10 days. Cultures were centrifuged at 2200xg for 10 minutes to isolate culture supernatants. Potential antimicrobial compounds were then extracted with ethyl acetate (Sigma-Aldrich), mixing solvent and culture supernatant in a 1:1 ratio at 300 rpm for 1 hour. After phase separation, the organic layer was collected and dried under airflow. Organic extracts were reconstituted in 500 µL of ddH_2O water and stored at -20˚C.

Antifungal susceptibility assays

Clinical and laboratory standard institute (CLSI) methods were used to assess the antifungal potential of *S. A28* extract and staurosporine or STS (Cayman Chemicals Co.) dissolved in DMSO (BioShop) (120). Briefly, a dilution range of the extract or pure STS was tested against 10^4 conidia/mL in RPMI 1640 without HEPES, phenol red, or glutamine (Wisent, Inc.). *Candida* and *Cryptococcus* inocula were prepared from a preculture of the fungi diluted in RPMI 1640 to an optical density at 600nm of 0.001 or 0.01, respectively. Plates were incubated at 37˚C, 5% CO_2 for 21 hours. Amphotericin B (Sigma-Aldrich) was dissolved in DMSO and used as a positive control.

Determination of fungal metabolic activity using the XTT assay was used to quantify antifungal susceptibility. To each well, 100 µL of RPMI 1640 and 50 µL a solution of 500mg/L of 2,3-Bis-(2-Methoxy-4-Nitro-5-Sulfophenyl)-2H-Tetrazolium-5-Carboxanilide) or XTT (BioShop) dissolved in ddH_2O water with 100 µM of menadione K3 (Sigma-Aldrich, Inc.) in ethanol (Greenfield Global) was dispensed into each well to reach a final volume of 250 µL. The XTT reaction was allowed a maximum of three hours at 37˚C 5% CO_2, and the absorbance at 450nm was measured using a spectrophotometer.

Fractionation of S. A28 extract

Fractionation began with 500 µL of the *S. A28* extract dispensed into a 1 mL hydrophilic-lipophilic-balanced (HLB) reverse phase column. The eluent H_2O:ACN (Fisher Scientific) with 0.1% trifluoroacetic acid (TFA) (Sigma-Aldrich) was added to the column 1 mL at a time, starting at 0% and increasing by 2% to 100%. Each fraction, 10 µL, was added to a flat-bottom 96-well plate (Grenier Bio-one) and lyophilized. *A. fumigatus* Af293 10^3 conidia in 100 µL of RPMI 1640 without phenol red or glutamine (Wisent, Inc.) was added to each well and then incubated for 21 hours at 37˚C 5% CO_2, after which antifungal susceptibility was quantified by the XTT assay as described above. Mass spectrometry (MS) was used to identify the ion within the elution fractions, each fraction of the *S. A28* extract was spotted on a matrix-assisted laser desorption/ionization time-of-flight (MALDI-TOF) steel plate in a ratio of 1:1 v/v with 5 mg/ml of α-Cyano-4-hydroxycinnamic acid (Sigma-Aldrich) reconstituted in 70% ACN. Mass spectra of each fraction were generated by Bruker Daltonics UltrafleXtreme MALDI-TOF in the positive mode, with a reflector and an accumulation of 5000 shots for the MS.

Identification of S. A28 extract active agent by high-resolution mass spectrometry analysis and molecular MS/MS

To identify ions within the active HLB elution fraction of the *S. A28* extract, an Agilent 1290 Infinity II Liquid Chromatography System coupled with a qTOF 6550 mass detector was used on the active fraction to record high-resolution mass spectra. Chromatographic separation was performed with a gradient mixture of H_2O (0.1% formic acid v/v) and acetonitrile (0.1% formic acid v/v) using a C8 column (Agilent). The gradient started at a ratio of 5% ACN with formic acid and then increased to 100% over the course of 7 minutes before the column was washed with the H_2O and formic acid reagent. With the mass detector set in the positive mode, data were collected from m/z 100–1700 with an acquisition rate of five spectrums per second. The ions of interest were selected by auto MS/MS scan fragmentation. The active agent was identified after MS/MS data was analysed by Global Natural Product Social molecular networking tools, filtering the ion fragments and matching the fragment pattern from the consensus spectra to that of known natural products (121).

The identification of STS as the compound responsible for the antifungal activity in the *S. A28* extract was confirmed with high-performance liquid chromatography, using a 15mm C-18 reverse phase column (Agilent) and H_2O:ACN with 0.2% formic acid as the eluent. The percentage of ACN was started at 5% for 5 minutes, and then gradually increased to 100% for a duration of 60min. This was coupled with UV-Vis spectroscopy at 292nm to quantify STS in a 1 in 20 dilution of the *S. A28* extract using a standard curve of commercial STS.

Confocal microscopy

10^3 conidia from a strain of *A. fumigatus* constitutively expressing green fluorescent protein (GFP), Af293::GFP, was used to inoculate 400 µL RPMI 1640 without HEPES, phenol red, or glutamine in 35mm uncoated dishes with glass coverslip (MatTek) and incubated at 37˚C 5% CO_2. 0.1 µg/mL of STS in DMSO was distributed at inoculation, 8 hours, or 18 hours after inoculation. After a 16-hour incubation, the microplates were counterstained with a 1 in 400 dilution of 1 mg/mL calcofluor white or CFW (Sigma-Aldrich) and analysed by the Zeiss LSM780 laser scanning confocal microscope and laser scanners with IR-OPO at an objective of 20X and 488nm.

Animal studies

Balb/c female mice (Charles River Laboratories) immunosuppressed with Ly6g antibodies (Cedarlane) were used for all experiments. Each mouse received 0.2mg of anti-mouse Ly6g antibodies by intraperitoneal (IP) injection every other day, starting a day before or on day -1, until the end of the study (122, 123). To determine the maximum tolerated dose, mice were given three intravenous (IV) treatments of 100 µL containing 0, 0.4, or 0.8 mg/kg STS in 10% DMSO in saline (ultrasonicated for one minute) on days 0, 2, and 4 and observed until day 7. Once the maximum tolerated dose was determined, a dose-response study of STS was conducted to determine the effects of STS on mouse survival during an *A. fumigatus* infection. Mice were rendered neutropenic by the Ly6g antibody regimen and then challenged with $5x10^6$ *A. fumigatus* Af293 6-day-old conidia, by a 50 µL intratracheal injection with $1x10^8$ conidia (122). STS at 0.1, 0.2, and 0.4 mg/kg was given intravenously (IV) 3 hours and 48 hours post-infection (PI). The physical symptoms and survival of the mice were monitored over 12 days.

The effect of STS on fungal burden was explored with quantitative histology. Mice immunosuppressed with Ly6g were infected with $5x10^6$ *A. fumigatus* Af293 6-day-old conidia, by a 50 µL intratracheal injection with $1x10^8$ conidia. An IV treatment of 0 or 0.4 mg/kg of STS with 10% DMSO in saline was administered at 3 hours and 24 hours PI. The mice were then sacrificed on day 2 PI and their lungs were harvested and fixed in formalin for three days before being embedded in paraffin blocks. Slices were taken from the lungs at 100 µm intervals and stained with Grocott's methenamine silver by the Histopathology Platform at the McGill University Health Centre. Samples were blinded for analysis and the number and area of pulmonary lesions were measured using QuPath image analysis software (124).

Phosphoproteomics

$8x10^8$ conidia of *A. fumigatus* Af293 were incubated in 400 mL of minimal media with or without 0.1 µg/mL of STS in DMSO at 37˚C and 200 rpm for 24 hours. The resulting biomass was harvested and suspended in ice-cold PBS with 0.1 mM Na_3VO_4, 1 mL/20g of protease inhibitor cocktail (BioShop Inc.), 5 mM NaPPi, and 1 mM DTT. The biomass was crushed with a Polytron® homogenizer (Kinematica) and NP-40 detergent was added to a final concentration of 1.75% v/v. After 1 hour of incubation at 4˚C, acetone precipitation of proteins was performed following the protocol provided by Thermo Fisher Scientific Inc. (125). Five biological replicates were collected before further processing. Isolation, enrichment, and analysis of phosphoproteins were performed by the Proteomics Platform at the McGill University Health Centre Research Institute Glen site. Phosphopeptides were identified using Scaffold 5 and the FungiDB database, and functionally categorized by FungiFun2 using the Gene Ontology (GO) method (126-128).

Gas chromatography analysis

$8x10^8$ *A. fumigatus* Af293 conidia was incubated in 400mL of minimal media with glucose at 37˚C and 200 rpm. Cultures were grown untreated or in the presence of subinhibitory concentrations of STS in DMSO or caspofungin in ddH_2O at 0.015625 µg/mL and 0.0625 µg/mL, respectively. Biomass from three biological replicates was harvested through filtration with Miracloth and reconstituted in 70% ethanol. Biomass was crushed in a 15 mL Potter-Elvehjem Tissue Grinder, suspended in 70% ethanol, and incubated in a 70˚C water bath for 15 minutes. The suspension was centrifuged at 2200xg to remove the supernatant, and the pellet was washed twice with ethanol. The pellet was then suspended in 40 mL of a 1:1 methanol:chloroform (Fisher Scientific) solution, and incubated on a nutator at room temperature overnight. The suspension was centrifuged to remove the methanol:chloroform solution and the pellet was resuspended in 40 mL of acetone and incubator on the nutator at room temperature for 2 hours. The pellet, now prepared cell wall, was centrifuged to remove the acetone and dried overnight in the fume hood (129).

Using Analytical Balance Precisa ES 320A, 0.5 mg of prepared cell wall from each condition was added to two sure-stop vials (Agilent). A calibration mix was prepared with 100 mM of each monosaccharide in ddH_2O: arabinose, rhamnose, fucose, xylose, mannose, galactose, glucose, glucuronic acid, N-acetylgalactosamine and N-acetylgalactosamine. Two calibration sets of 10, 50, 100, 250, and 500 µL of the calibrant mix were dispensed into sure-stop vials. Each sure-stop vial was spiked with 10 µL of 10 mM D-(+)-chiro-inositol in ddH_2O, and calibration set vials were placed under the sample concentrator to dry. One set of sample vials and a calibration set received 250 µL of 6M HCl in ddH_2O, and 250 µL of 2M TFA in ddH_2O was dispensed into the remaining set of vials. The vials were capped and incubated at 110˚C for 2 hours. The vials with TFA were

removed and placed under the sample concentrator. The vials with HCl were incubated for an additional 2 hours at 100˚C, followed by evaporation by the sample concentrator. Once the vials were completely dried, 100 µL 1M of hydrogen chloride in methanol (Sigma-Aldrich) was dispensed into every vial and incubated at 80˚C overnight (129).

After methanolysis, the vials were again evaporated under the sample concentrator. The vials were washed with 500 µL of methanol followed by evaporation, twice, before 600 µL of 5:1 methanol:pyridine was added to each vial. This was followed with 150 µL of acetic anhydride (Fisher Scientific), after which the vials were quickly capped and incubated at room temperature for 1 hour. The vials were then evaporated and washed with methanol twice before 50 µL TriSil-HTP reagent (Thermo Fisher Scientific) and incubated at 110˚C for 20 minutes. The TriSil HTP mix was evaporated and the vials were washed twice with 500 µL cyclohexane (Sigma-Aldrich). The vials were reconstituted with 1mL of cyclohexane before being placed in the autosampler of the Gas Chromatography Mass Spectrometer or GC-MS (Agilent). The injection volume was 1 µL for each sample and calibrant, with a blank injection of pure cyclohexane in between. The GC method started at 120˚C for 2min, 120˚C to 160˚C for at 15˚C/min, 160˚C to 195˚C at 1.5˚C/min, 195˚C to 280˚C at 30˚C/min, then 280˚C was held for 1.5min. The MS was scanned starting at t=6min from m/z 50 to 400 every 4.1 scans/second (129).

Glucan polymer quantification

The prepared cell wall, previously used for the GC analysis, was solubilized in dH_2O and then boiled at 95˚C for 15 minutes, followed by an overnight suspension in 1M NaOH (BioShop) with 0.2 g/L $NaBH_4$ (BioShop) on the nutator. The solutions were then neutralized with HCl, separating branched β-(1,3)-D-glucan and α-glucans in the neutral-soluble fraction and neutral-

insoluble fraction respectively (130, 131). These glucans were separated by centrifugation at 2200xg, then dried and stored at room temperature.

β-(1,3)-D-glucan quantification was performed using the Glucatell® endpoint assay (132). The neutral soluble fraction from each condition described above was reconstituted in 1M NaOH, which was then used to prepare 0.5-4 µg/mL solutions with the LAL water from the Glucatell kit. The Glucatell assay was performed according to the package insert with the prepared sample glucan solutions (132).

The relative abundance of α-glucans was quantified by enzyme-linked immunosorbent assay (ELISA). A 384-well Immulon 4 HBX microplate was incubated overnight at room temperature with 20 µL of serial 1/4 dilutions starting at 1 mg/mL of the neutral-insoluble fraction described above suspended in 1M NaOH. After three washes with 100 µL of Tris-Buffered Saline (TBS-T) with 0.5% of Tween-20 (BioShop), the plate was first incubated with 2.5 µg/mL of anti-α-glucan mouse IgM monoclonal antibody in TBS-T as the primary antibody, followed by a coating with a 1 in 1,000 dilution of anti-mouse IgM HRP-conjugated secondary antibody. TBS-T washes were performed between each step. The signal was quantified by measuring the 450nm absorbance from the TMB reaction (Millipore) stopped with 1M H_2SO_4.

Results

S. A28 culture supernatant extracts exhibit potent antifungal activity against a panel of human fungal pathogens

As the *S. A28* culture supernatant extract exhibited antifungal activity against fungi that cause dairy spoilage, we sought to determine if the extract was also active against human fungal pathogens. The antifungal activity of *S. A28* extracts was tested against the three common human fungal pathogens, *A. fumigatus*, *R. oryzae*, and *C. albicans,* following standard CLSI microbroth dilution methods (Fig. 1A). As the composition of these extracts was unknown at the time of testing, the inhibitory concentration of crude *S. A28* extract required to reduce the metabolic activity of the fungi by 50% (IC_{50}) was expressed as a function of the extract dilution (1/dilution factor, Fig. 1A). All three fungi were found to be sensitive to *S. A28* extract at concentrations above a 1/10 dilution (Fig. 1A). *A. fumigatus* seemed to be the most affected by the extract with a mean IC_{50} below 0.01 arbitrary units (1/100 dilution, Fig. 1A). The IC_{50} of *S. A28* extract against *R. oryzae* and *C. albicans* were higher at 0.04 and 0.05 arbitrary units, respectively (Fig 1A). These findings suggest compounds present in the *S. A28* extract are active against human fungal pathogens.

The antifungal active component of the S A28 cultures supernatant extract is staurosporine (STS)

Given the antifungal activity of the *S. A28* extract, we next set out to identify the active antifungal compound(s) within this preparation. Fractionation of the *S. A28* extract was performed by liquid chromatography using a reverse-phase hydrophilic-lipophilic balanced (HLB) column to isolate semi-purified fractions for antifungal activity analysis. Determination of the antifungal activity of each fraction was determined by susceptibility testing against *A. fumigatus*, and fractions exhibiting antifungal activity were then subjected to matrix-assisted laser

desorption/ionization time-of-flight mass spectrometry (MALDI-TOF MS) analysis to characterize the composition of relevant fractions. Antifungal activity was found to be concentrated within the fractions eluted with 24-28% ACN with 0.1% TFA (Fig. 1B). Analysis of these fractions by MALDI-TOF MS showed that all fractions with antifungal activity contained an ion at 467 m/z (Fig 1B). The semi-purified fractions containing this ion were then analysed by liquid chromatography-mass spectrometry and comparison to their library of identified natural products by our collaborators at the Wright Lab (McMaster University). The mass of the 467 m/z ion, its retention time based on liquid chromatography, and the MS/MS fragment pattern all matched that of STS, a broad-spectrum kinase inhibitor first isolated from a *Streptomyces* species in Japan (Fig. S1) (133). STS is a non-specific protein kinase inhibitor and was previously investigated as an anti-cancer agent but has not been evaluated as an antifungal (133, 134). To confirm this identification, high-performance liquid chromatography (HPLC) was used to calculate the concentration of STS within *S. A28* extracts and the antifungal activity of these extracts compared with that of purified commercial STS. STS solutions 1 to 25 µg/mL in ddH_2O water, using a stock solution in DMSO, were assayed by HPLC to generate a standard curve, followed by analysis of a 1 in 20 dilution of *S. A28* extract. The *S. A28* extract tested was found to have 83µg/mL of STS (Fig. S2), confirming STS as the compound responsible for the observed antifungal activity of the extract.

Commercial staurosporine has potent antifungal activity

Following the identification of STS as the active agent in the *S. A28* extract, commercial STS was used for future studies, including antifungal susceptibility assays against an expanded panel of human fungal pathogens. At the molar level, STS was found to be as effective as amphotericin

B, and even more active against some fungal pathogens such as *A. fumigatus* (0.3 vs 1.5 μM, $P = 0.0159$, Fig. 1C). As with other antifungals, STS was least active against *C. auris* but was still significantly more effective than amphotericin B (1 vs 6 μM, $P < 0.0001$, Fig. 1C). Since *A. fumigatus* was the most sensitive fungi from this screen, it was chosen as the model organism for further studies of the antifungal activity of STS.

The antifungal effect of STS on the growth and viability of *A. fumigatus* at different stages of the fungal life cycle was investigated by confocal microscopy using a strain of *A. fumigatus* producing green fluorescent protein (GFP) (Af293::GFP). The use of this strain allows for the detection of fungal viability, as cytosolic GFP signal is lost upon fungal death (135). Following exposure to STS and 16 hours of growth, fungi were stained with CFW to visualize biomass, and imaged by confocal microscopy. Incubation of *A. fumigatus* conidia and germlings with 0.1 μg/mL of STS resulted in complete inhibition of fungal growth (Fig. 2). Dormant conidia grown for 16 hours in the absence of STS matured into a young hyphal biofilm, yet in the presence of STS only conidia were observed. The majority of STS-exposed conidia that were only positive for CFW had diameters larger than the typical 2-3μm range, indicating they had entered the swollen conidia stage (118). Still, due to the absence of germ tubes these conidia had likely failed to complete germination before undergoing cell death (Fig. 2). A minority of conidia remained positive for GFP and had produced very short germ tubes, indicating they were arrested at the early germination stage (Fig. 2). For the germlings, STS seemed to arrest growth at the young hyphae stage, while the untreated control formed a mature hyphal biofilm. The majority of STS-exposed germlings were CFW-positive only, indicating they were killed (Fig. 2) Two staining patterns were observed in the rare GFP-positive germlings; some germlings were entirely GFP-positive, thus still alive but exhibited arrested growth. Other germlings only had a GFP-positive hyphal subsection present

between two septa, suggesting that the majority of segments within the filamentous septated hyphae had been killed but that a single segment within the young hyphae still survived possibly by closing the septal pore (Fig. 2). The biofilm treated with STS had a much higher number of GFP positive cells, with only segments of hyphae appearing to be dead, suggesting the concentration of STS used was subinhibitory against a mature biofilm. The growth of the biofilm, however, appeared to be less dense and to contain fewer branching hyphae compared to the untreated control (Fig. 2). Overall, STS was most effective at the earlier stages of fungal growth, with more conidia and germling death, but still had a visible antifungal effect against a biofilm at a subinhibitory concentration.

Staurosporine has a low therapeutic index but can protect mice against invasive aspergillosis at sub-toxic doses

STS has been extensively investigated as an anti-cancer agent, but tolerability issues due to its non-specific kinase inhibitory activity have limited its success in human clinical trials (136). Furthermore, STS has been shown to induce apoptosis in leukocytes, raising concerns about its effect on host immunity (137, 138). We, therefore, sought to characterize the therapeutic index of STS by comparing the susceptibility of fungi and human cells to this agent. Cytotoxicity assays were performed against the human A549 cell line and the IC_{50} was calculated based on the viability of the cells as measured using the metabolic MTT assay. We found there was around a 2-fold difference between the IC_{50}s against the A549 cell line and most of the fungal pathogens in the tested panel (Fig. 3). This narrow therapeutic index suggested that identifying a non-toxic dose of STS that mediates antifungal efficacy may be challenging to find *in vivo*.

Due to the observed cytotoxicity of STS at relatively low concentrations relative to those required for antifungal activity, we sought to evaluate the antifungal and tolerability of chemical derivatives of STS, which were originally developed to increase the specificity of the kinase inhibitory activity for cancer therapy (139). Many of these derivatives have been observed to exhibit lower cytotoxicity than the parent compound (140). We hypothesized that some of these less toxic agents may exhibit retained antifungal activity and therefore have their improved potential for development as antifungal agents compared to STS. However, of the eleven STS derivatives tested, only UCN-01 and K252a retained antifungal activity (Fig. 3). UCN-01 had a significantly higher IC_{50} relative to STS not only against A549 cells (2 vs 0.5 μM, $P = 0.0018$), but also against several of the fungal pathogens including *A. fumigatus* (8 vs 0.3 μM, $P = 0.0023$), *R. oryzae* (2 vs 0.2 μM, $P = 0.0225$), and *C. albicans* (1.5 vs 0.3 μM, $P = 0.0179$). The IC_{50}s of K252a were non-significant compared to that of STS against the entire panel. Both derivatives had similar therapeutic indices to their parent molecule (Fig. 3). We therefore elected to focus on STS for future experiments.

To determine if STS could exhibit antifungal activity at tolerable doses *in vivo*, we explored the tolerability and efficacy of STS in a mouse model of invasive aspergillosis. We first sought to determine the maximum tolerated dose of intravenous STS in mice (141). As STS was dissolved in 100% DMSO for *in vitro* experiments, we first identified an appropriate intravenous vehicle with no more than 10% DMSO (142). STS was found to be soluble and retained *in vitro* activity when dissolved in 10% DMSO in saline. To determine the maximum tolerated dose of STS in this vehicle, experiments were performed to evaluate the tolerability of 0.4 and 0.8 mg/kg of STS in neutropenic mice. The maximum tolerated dose of STS was 0.4mg/kg of STS, above which the mice displayed behavioural signs of distress such as burrowing as a group and attempting to hide

or flee when we attempted to pick them up. We therefore decided to proceed with doses at or below 0.4 mg/kg for future efficacy studies.

To characterize the *in vivo* efficacy of STS, we tested the effects of a range of STS concentrations (0.1-0.4 mg/kg) in a mouse model of invasive aspergillosis (122). Mice were immunosuppressed by neutrophil depletion with Ly6g treatment, then infected with $5x10^6$ conidia of *A. fumigatus* Af293 by intratracheal inoculation. Mice were then observed, or treated with STS by IV 3 hours and 48 hours PI and monitored for body weight, temperature, and survival for 14 days. These dose-response experiments demonstrated increased survival of the mice with increasing doses of STS (Fig. 4A). Treatment with 0.1 mg/kg of STS was ineffective. The treatment with 0.2mg/kg of STS led to a trend towards increased survival but was not statistically significant as compared with untreated mice (60% vs 40%, respectively, Fig. 4A). Treatment with 0.4mg/kg of STS resulted in a statistically significant increase in mouse survival as compared with untreated controls (70% vs 40%, $P = 0.0005$, Fig. 4B).

To confirm that the improved survival with STS treatment was a consequence of direct antifungal activity rather than any effect of STS on host cells, we examined the effects of STS treatment on the pulmonary fungal burden of *A. fumigatus*-infected mice treated with STS. Fungal burden was quantified with quantitative histopathology using Grocott's methenamine silver (GMS)-stained mouse lung slides. The slides were prepared from lungs harvested from infected mice on day 2 PI. Blinded samples were reviewed and lesions or areas with visible fungal growth were identified. The number and the area of lesions were quantified using the bioimaging analysis application QuPath. A lower median number of lesions per mouse lung treated with STS compared with untreated mice (2 vs. 12 lesions per mouse lung, Fig. 4C), although not statistically significant. The lesions in the lungs of untreated mice also exhibited a greater range in area compared to those

in the STS-treated lungs (with a maximum at 80 vs 40mm^2, respectively), with a non-significant difference in the average area (Fig. 4D). Taken together, the results of the survival and quantitative histopathology studies suggest that STS is an effective antifungal *in vivo* and directly acts against *A. fumigatus,* reducing the pulmonary fungal burden.

Staurosporine down-phosphorylates CWI pathway proteins and cell wall polymer synthases

In light of this promising *in vivo* data, we sought to better understand the mechanism of action for STS within fungi. Given STS is a broad-spectrum kinase inhibitor, we chose to investigate its effect on the phosphoproteome of *A. fumigatus*. Proteins were extracted from 24-hour-old *A. fumigatus* exposed to a subinhibitory concentration of STS or buffer alone and then subjected to phosphoproteomic analysis as an unbiased approach to identify STS-dependent differences in protein phosphorylation. As expected, exposure of *A. fumigatus* to STS was associated with a general trend of protein down-phosphorylation, although several proteins were found up-phosphorylated or phosphorylated only in the presence of STS (Table 1). Functional categorization of the identified phosphopeptides by FungiFun2 revealed that the most impacted protein groups labeled with GO terms included cytosolic proteins, hyphal growth, and cellular response to drugs. (Fig. 5A). Other proteins not covered by GO terms included DNA and RNA binding proteins, multi-drug transporters, and proteins involved in nitrogen metabolism (Fig. 5A).

Additionally, a number of changes in phosphoprotein abundance were identified in the cell wall integrity (CWI) pathway, and proteins involved in cell wall glycan synthesis (Fig. 5A). Three CWI pathway proteins were found to be down-phosphorylated in response to STS exposure, including: the cell wall stress sensor Wsc1, *Aspergillus* protein kinase C PkcA, and mitogen-activated protein kinase Bck1. Unexpectedly, we also found that a transcription factor activated by

the CWI pathway, RlmA, was phosphorylated with STS exposure. RlmA is known to upregulate the transcription of several cell wall glycan synthase genes: β-(1,3)-D-glucan synthase *fks1*, α-glucan synthase *ags1*, and three chitin synthases *chsE*, *chsF,* and *chsG* (72). Interestingly, the protein products of these RlmA-dependent genes (Fks1*,* Ags1*,* ChsE, ChsF, ChsG, and another chitin synthase CsmB and chitin synthase activator Chs3) were all down-phosphorylated upon exposure to STS (143). Collectively these results suggest that STS exposure may have significant effects on fungal cell wall composition, which may contribute to the antifungal effects of this agent.

Staurosporine decreases β-(1,3)-D-glucan content in the A. fumigatus cell wall

The results of the phosphoprotein analysis raised two key questions about the effects of STS on cell wall glycan composition. First, what is the net effect of the down-phosphorylation of CWI proteins and the activation of the downstream RlmA on the CWI pathway, and consequently, the production of chitin? Second, what is the net impact of these effects on the CWI pathway and the down-phosphorylation of cell wall glycan synthases on cell wall composition? With these two questions in mind, we subsequently turned to chemical and molecular techniques to study the effects of STS exposure on *A. fumigatus* cell wall composition.

To determine the net effects of STS-dependent down-phosphorylation of CWI proteins and activation of RlmA on the state of the CWI pathway, we determined the effects of STS exposure, at 0.08 times the minimum inhibitory concentration (MIC), on fungal N-acetylglucosamine (GlcNAc) content. *A. fumigatus* treated with a sub-inhibitory concentration of caspofungin (a known activator of the CWI pathway), at 0.25 times the minimum effective concentration (MEC), was used as a positive control (66). Cell wall extracts were derivatized and analysed by gas chromatography-mass spectrometry (GC-MS). As expected, treatment with caspofungin resulted

in a significant increase in cell wall GlcNAc content as compared to the untreated *A. fumigatus* (1.7 vs 1, $P = 0.005$, Fig. 5B). No increase in chitin was observed in *A. fumigatus* exposed to STS, although substantial variation between the biological replicates was observed (1.17 vs 1, Fig. 5B). The lack of a consistent increase in chitin content upon STS exposure suggests the down-phosphorylated CWI proteins and/or reduced phosphorylation of chitin synthases are dominant, and that the CWI pathway is not activated in response to STS exposure.

In addition to the effects on CWI pathway proteins, STS exposure was associated with the down-phosphorylation of Fks1. The specific phosphopeptides identified by this analysis were found to be within the accessory domain of Fks1, a location in which mutations have been described to impact enzyme function (144). We therefore hypothesized this down-phosphorylation could lead to lower Fks1 activity and by extension, lower β-(1,3)-D-glucan content in the cell wall. To distinguish β-(1,3)-D-glucan from α-glucans, the amount of branched β-(1,3)-D-glucan was measured using the Glucatell® endpoint assay. Glucans extracted from *A. fumigatus* biomass treated with a subinhibitory concentration of the Fks1-inhibitor caspofungin were used as a positive control. As expected, when normalized to cell wall extract mass, a significant decrease in β-(1,3)-D-glucan content was observed in the caspofungin-treated *A. fumigatus* cell wall extract as compared to the untreated control (0.3 vs 1, $P = 0.017$, Fig. 5C). Similarly, a trend to a decrease in β-(1,3)-D-glucan content was observed in the STS-treated *A. fumigatus* cell wall, as compared to the untreated control (0.5 vs 1, Fig. 5C). This difference was not significant, however, and further replicates are required to confirm that STS inhibits Fks1 activity.

The phosphoproteomic analysis also revealed the α-glucan synthase Ags1 to be down-phosphorylated in *A. fumigatus* with STS exposure. To measure the effect of STS exposure on α-glucan cell wall content, the relative abundance of α-glucans was determined by ELISA in the

same cell wall extracts of STS-treated, caspofungin-treated, and untreated *A. fumigatus*. As expected, caspofungin treatment had no significant α-glucan content change as compared to the untreated control (1.18 vs 1, Fig. 5D). There was also no significant change in α-glucan content with STS exposure as compared to untreated control (1.04 vs 1, Fig. 5D). These results suggest that STS exposure has little direct impact on α-glucan content in the *A. fumigatus* cell wall despite down-phosphorylation of Ags1.

Staurosporine synergizes with echinocandins against A. fumigatus in vitro

As we previously found STS exposure resulted in the down-phosphorylation of Fks1, and a trend to a reduction in β-(1,3)-D-glucan content in the *A. fumigatus* cell wall, we hypothesized STS could potentiate the activity of echinocandins, whose primary mechanism of action is the inhibition of Fks1 (145). We, therefore, tested STS in combination with the echinocandins caspofungin and micafungin. Checkerboard assays were performed to confirm the potentiation of echinocandin activity by STS, and a Fractional Inhibitory Concentration Index (FICI) was calculated to define the interaction between the two drugs. We observed the potentiation of antifungal activity for caspofungin and micafungin against *A. fumigatus* in the presence of STS at sub-cytotoxic concentrations (Fig. 6A-B). The FICIs were below 0.5, the threshold for synergistic interaction, suggesting that STS synergizes with both caspofungin and micafungin against *A. fumigatus in vitro*. As a control, STS was also tested in combination with the azole antifungals itraconazole and voriconazole, which have no effects on Fks1 and do not trigger the CWI pathway (146). No potentiation of activity was observed with combinations of azoles and STS, suggesting that the synergy observed with STS and echinocandins was class-specific (Fig. 6C-D). We further evaluated the combination of echinocandins and STS against a set of *Candida* species, pathogens

commonly treated with echinocandins, and *C. neoformans,* which is constitutively resistant to echinocandins and largely lacks β-(1,3)-D-glucan (Table 2) (109, 147). Unlike *A. fumigatus*, synergy of STS with either caspofungin or micafungin was not consistently effective among *Candida* species tested (Table 2). Caspofungin and STS were synergistic against *C. albicans*, *C. auris*, *C. tropicalis,* and *C. glabrata*, yet *C. auris* was the only *Candida* species that micafungin and STS were synergistic against (Table 2). There was no potentiation between STS and echinocandins observed against *C. neoformans*, which was not unexpected as echinocandins are ineffective against this pathogen due to intrinsic resistance (Table 2) (147). Overall, the echinocandin and STS combination was most effective in *A. fumigatus*, thus we chose this pathogen for further efficacy studies *in vivo*.

Staurosporine and caspofungin combination therapy may be synergistic in vivo

Combination STS-echinocandins therapy could offer several advantages. The use of caspofungin could allow for the use of a reduced STS dose, and therefore lower the chances of STS toxicity. Although 0.4mg/kg of STS was effective as a monotherapy for invasive aspergillosis in mice, there was still an up to 30% mortality rate in treated animals, which could potentially be improved with combination therapy. To evaluate if the synergy between STS and echinocandins could be reproduced *in vivo*, the combination of subtherapeutic doses of STS and caspofungin was evaluated in the mouse model of invasive aspergillosis. A dose of 0.5 mg/kg caspofungin was selected as this has been previously established as a sub-therapeutic concentration in this model (148). STS at 0.2mg/kg was selected based on the previous dose-response experiment (Fig. 4A). Monotherapy with STS increased mouse survival rates compared with untreated controls (60% vs 30% for untreated mice, $P = 0.0008$, Fig. 7). Similarly, caspofungin monotherapy was associated

with an increase in mouse survival compared with untreated controls (50% vs 30%, $P = 0.022$, Fig. 7). The combination of 0.5mg/kg caspofungin with 0.2mg/kg STS did increase survival rates compared to the untreated control (80% vs 30%, $P = 0.0006$, Fig. 7). The combination, however, only had a small significant increase relative to caspofungin monotherapy (80% vs 50%, $P = 0.04$), and no statistical difference relative to STS monotherapy (80% vs 60%, Fig. 7). Taken as a whole, although some improvement in outcomes was observed with the combination of lower dose caspofungin and STS compared with monotherapy with either agent alone, further studies are required to determine if this is biologically and clinically significant.

Discussion

In this work, we demonstrated that an organic extract of culture supernatants produced by *S. A28* exhibits antifungal activity against several human fungal pathogens. The active agent responsible for this activity was identified as STS, a broad-spectrum kinase inhibitor. At the molar level, STS was as effective against multiple human fungal pathogens compared to amphotericin B and synergized with the echinocandin caspofungin *in vitro*. Phosphoproteomic studies identified significant alterations in the phosphoproteome of STS-exposed hyphae, including multiple proteins involved in cell wall synthesis. STS treatment resulted in improved survival in mice infected with *A. fumigatus* and infected mice treated with the combination of caspofungin and STS exhibited a trend towards improved survival compared with monotherapy with either agent.

Most literature on STS activity details its anticancer activity, but there have been few studies exploring the antifungal efficacy of this agent and its potential mechanism of action in fungi. When STS was first discovered in 1977, it was found to have activity against multiple fungi including *A. fumigatus* and *C. albicans*, which is consistent with the susceptibility assays testing the *S. A28*

extract and commercial STS, however further development of STS as a therapeutic was not pursued (133). As a kinase inhibitor, STS has been used as a tool to investigate druggable targets of virulence and drug resistance in *C. albicans* (149, 150). Aligned with our findings, synergistic interactions between STS and antifungals have been previously reported *in vitro*: STS synergized with micafungin, fluconazole, and terbinafine in *C. albicans,* which the researchers attributed to inhibition of the *Candida* protein kinase C, Pkc1, as it is the primary target of STS (149, 151-153). The conclusion from this work was that reduction of Pkc1 activity increases sensitivity to agents that perturb the cell membrane and enhance the cidality of normally fungistatic drugs (149). We failed to duplicate these findings exactly, although we did observe synergy with caspofungin against *A. fumigatus*. Our phosphoproteomic work also suggests that STS has a much larger impact on fungal metabolism than simply reducing PkcA activity.

As the primary target of STS is protein kinase C, we had hypothesized that STS might largely mediate its effects though inhibiting PkcA, and enhanced echinocandin activity by inhibiting the compensatory upregulation of the CWI pathway in response to echinocandin treatment (151). Indeed, we found that not only was PkcA down-phosphorylated with STS exposure, but another kinase Bck1, and the cell wall sensor Wsc1 were also down-phosphorylated. Surprisingly, however, RlmA exhibited phosphorylation in response to STS exposure. RlmA is known to be involved in other stress responses aside from the CWI pathway, such as tolerance to oxidative damage, thereby suggesting that activation of RlmA via a non-canonical CWI pathway could activate downstream CWI effectors in the absence of PkcA, Bck1, and Wsc1 activation (72). However, the lack of increase in chitin (as determined by cell wall GlcNAc content) in response to STS exposure, suggests that the down-phosphorylation of the CWI proteins and downstream chitin synthases dominates over the potential activation of RlmA. Phosphorylation of chitin synthases is known to

impact enzyme localization and function, for example, in *Aspergillus nidulans* phosphorylation of the N-terminal is key for the efficient transport of chitin synthase ChsB to the hyphal apical surface (154). It is possible through down-phosphorylation, STS impacted the localization and function of ChsE, ChsF, ChsG, and CsmB in *A. fumigatus*.

Given the lack of changes in cell wall chitin in response to STS exposure, a more plausible explanation for the observed synergy of STS and the echinocandins may relate to the direct effects of STS on Fks1 and subsequent β-(1,3)-D-glucan cell wall content. It is currently unknown if phosphorylation of Fks1 impacts enzyme function, however, mutations in the domain where the phosphopeptides were identified have been shown to reduce enzyme activity (144). Our findings of a trend to lower β-(1,3)-D-glucan cell wall content following STS exposure suggests that this could be one mechanism whereby STS mediates antifungal activity, and synergizes with the Fks1 inhibitor caspofungin. The fact that the synergy of this combination was less marked *in vivo* could be attributed to two factors. First, monotherapy with 0.2mg/kg STS produced a significant survival benefit, making it more challenging to detect the synergistic effects of the combination therapy. Secondly, the *in vivo* conditions are completely different compared to the *in vitro* conditions from which the synergy was first observed, due to the pharmacodynamics related to the different modes and times of administration for each drug. Thirdly, STS could have affected the host immune system, as only neutrophils were depleted, and STS is known to impact the leukocytes that would have been present (137, 138). Testing of lower STS concentrations, and optimization of combination treatment will need to be undertaken to test these hypotheses. Finally, animal studies were conducted exclusively with female mice, sex differences should be considered and the experiments should be repeated with male mice as well. For example, as it has been shown there

are sex differences in the immune response to *A. fumigatus*, but sex differences have not yet been identified in the treatment of invasive aspergillosis (155).

This project highlights one of the limitations of traditional antimicrobial discovery, the risk of rediscovering small molecules, yet also emphasizes how screening known natural products with limited reported antifungal data could lead to the development of novel therapeutics. Our studies demonstrate the *in vitro* and *in vivo* antifungal activity of STS and suggest a possible role for this agent in combination with echinocandins. Future studies are required to better characterize the potential of STS as a therapy alone, and in combination with echinocandins, including more detailed toxicity studies and evaluating the effects of STS on the activity of echinocandins against echinocandin-resistant strains of *A. fumigatus*. Further investigation into elucidating the key molecular targets of STS that mediate its antifungal effect could also open the door to future structure-function studies to identify more specific kinase inhibitors with increased antifungal activity and reduced off-target effects.

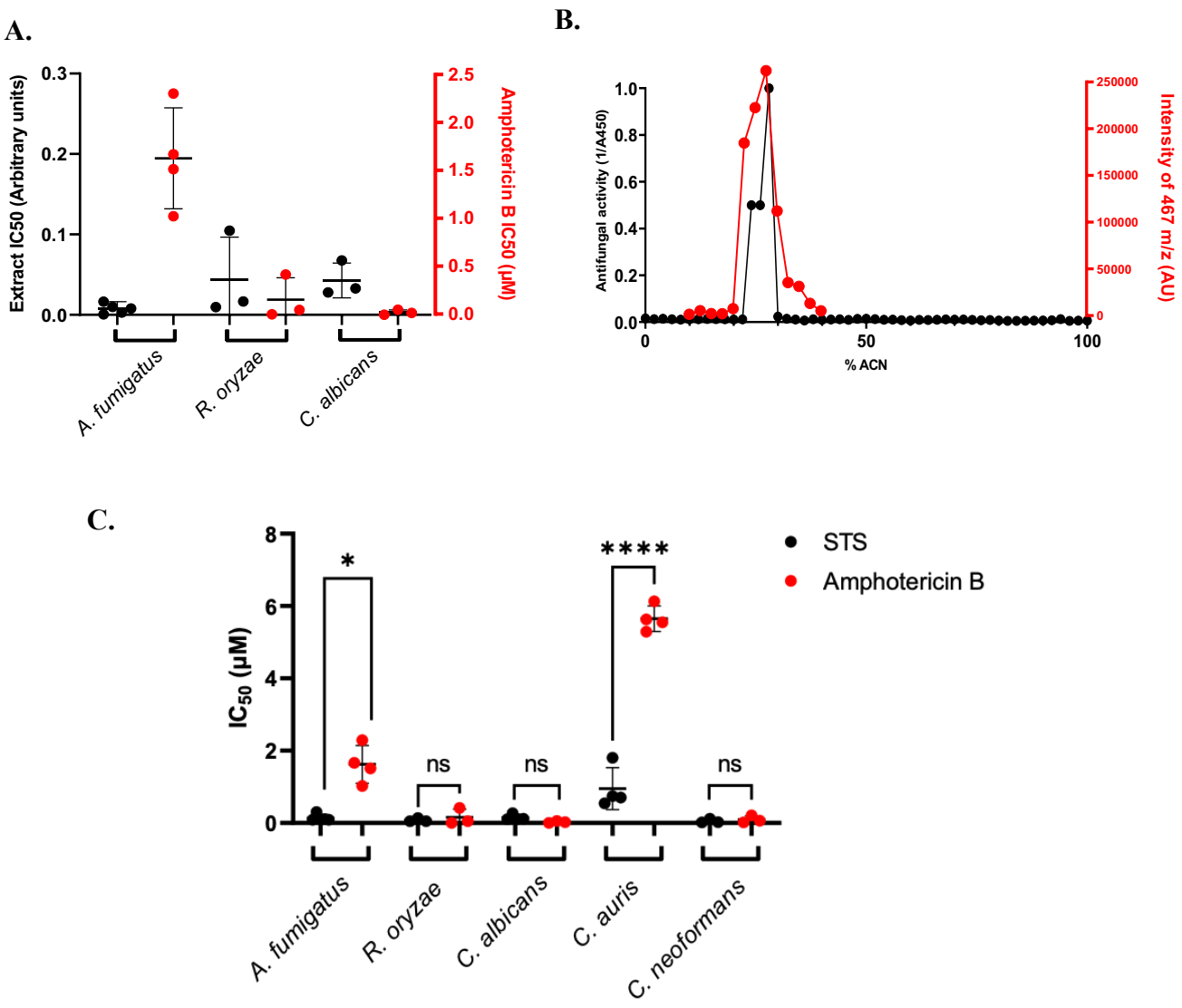

Figure 1: The S. A28 culture supernatant extract exhibits potent antifungal activity against multiple human fungal pathogens due to the presence of staurosporine

A: Antifungal activity of the organic extracts of *S. A28* supernatants (as indicated by IC_{50}) were determined against a panel of human fungal pathogens, with amphotericin B as a control. Each point represents a unique biological replicate (N = 3), and the dash indicates the mean and the error bars the standard deviation.. A ten-fold dilution of the *S. A28* extract is indicated as 0.1 arbitrary unit.

B: HLB elution fractions of the *S. A28* organic extract were tested for antifungal activity against *A. fumigatus*. Antifungal activity is indicated as the inverse absorbance at 450nm (a measure of fungal metabolism). The intensity of the 467 m/z ion as determined by MALDI-TOF MS was overlaid with antifungal activity for each fraction. The figure shown is a representative result of 3 independent replicates performed with unique *S. A28* extracts.

C: The antifungal activity of commercial STS in DMSO compared with amphotericin B against an expanded panel of fungal pathogens, with the dash representing the mean, with each point representing a replicate (N=3). The error bars represent the standard deviation. The significant difference between the *A. fumigatus, R. oryzae,* and *C. albicans* IC_{50}s is indicated (*, $P < 0.05$) relative to STS exposure as determined by the Mann-Whitney test due to lack of Gaussian distribution. The significant difference between the *C. auris and C. neoformans* IC_{50}s is indicated (****, $P < 0.0001$) relative to STS exposure as determined by the unpaired t-test.

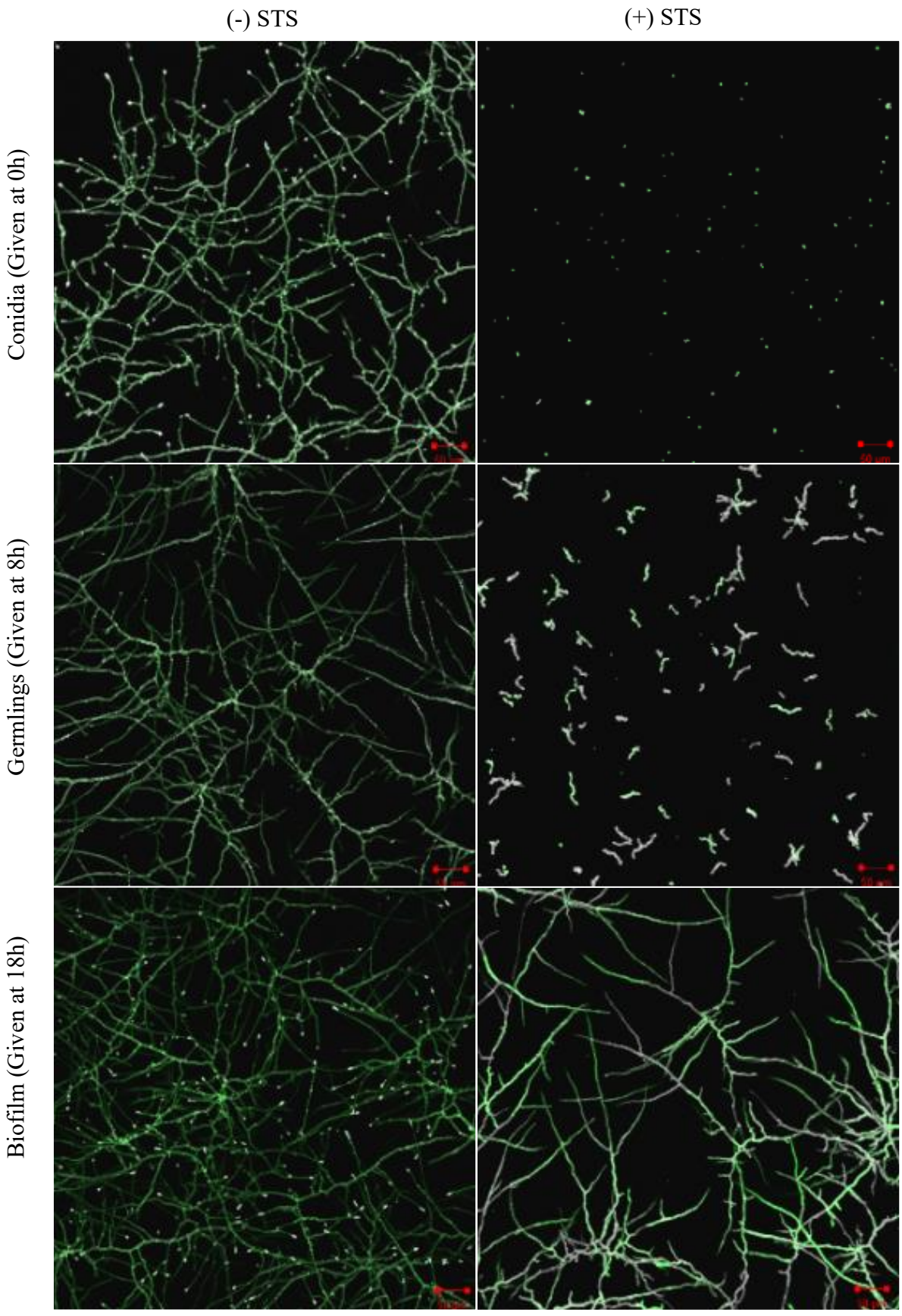
(-) STS
(+) STS
Conidia (Given at 0h)
Germlings (Given at 8h)
Biofilm (Given at 18h)

Figure 2: Staurosporine exhibits fungicidal antifungal against A. fumigatus that is most marked in conidia and young hyphae

GFP-expressing *A. fumigatus* wild-type strain (green) was grown in RPMI 1640. The growth stages tested included dormant conidia (0h of growth), young germlings (8h of growth), and hyphal biofilm (18h of growth). Samples were then further grown for 16 hours at 37˚C in 5% CO_2 with or without 0.1 µg/mL of STS. Organisms were counterstained with a 1 in 400 dilution of CFW (white) before confocal microscopy analysis at an objective of 20X. Images are a merge of the two stains, with single-stain images in supplementary. Images shown are from a single representative experiment of three independent replicates.

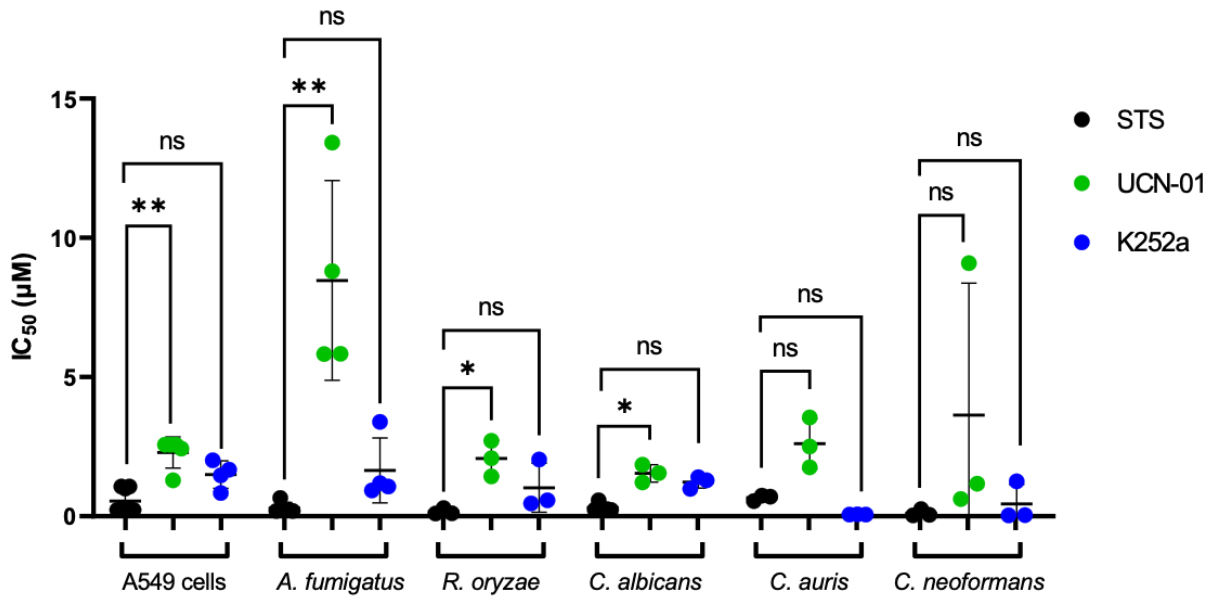

Figure 3: Staurosporine derivatives UCN-01 and K252a have reduced antifungal activity than the parent molecular but remain cytotoxic.

The antifungal and cytotoxic activity of STS derivatives, UCN-01 and K252a, against a panel of fungal pathogens and the human A549 cell line (x-axis) was assessed in comparison to the parent molecule STS. Antifungal microbroth dilution assays were performed using CLSI standards, and serial dilutions of STS and its derivatives were tested against 10,000 A549 cells to assess cytotoxicity. The IC_{50} (y-axis) was determined by measuring the metabolic activity of fungal pathogens, as determined by the XTT assay, or the viability of the cells measured by the MTT assay. Results are from independent experiments with N = 3 at minimum per drug and fungal pathogen combination, displaying the mean, and error bars represent the standard deviation. The significant difference is indicated within each fungal pathogen relative to STS exposure (*, $P < 0.05$) as determined by the Kruskal-Wallis multiple comparisons test.

A.

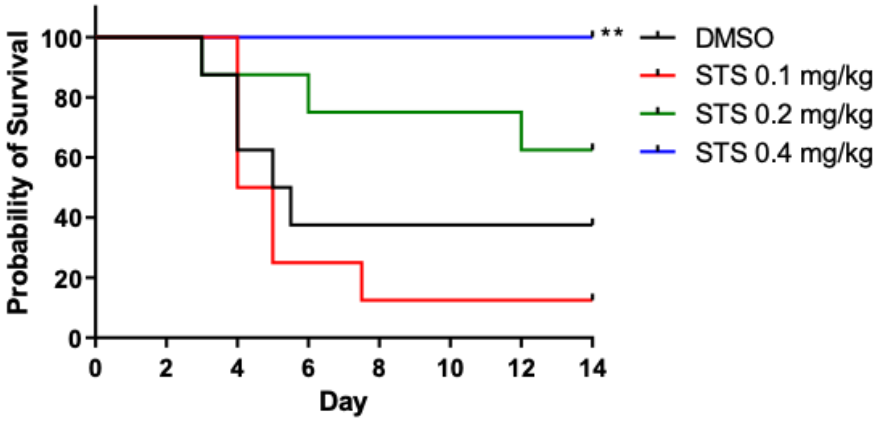
Probability of Survival
100
80
60
40
20
0
0
2
4
6
8
10
12
14
Day
**
DMSO
STS 0.1 mg/kg
STS 0.2 mg/kg
STS 0.4 mg/kg

B.

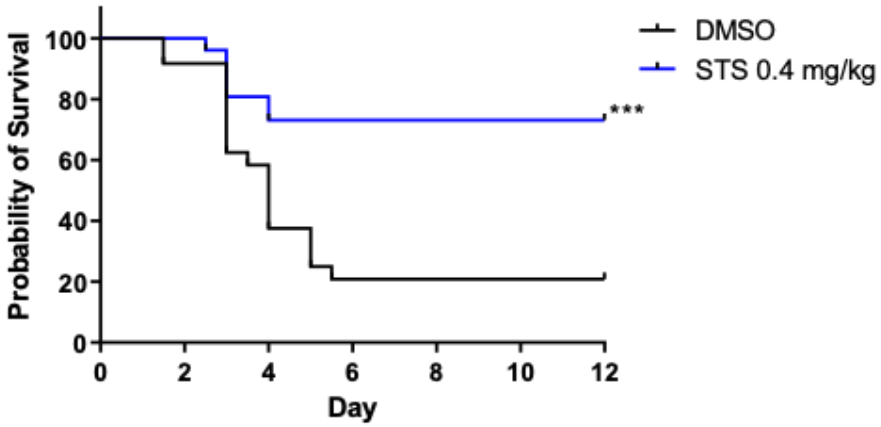
Probability of Survival
100
80
60
40
20
0
0
2
4
6
8
10
12
Day
***
DMSO
STS 0.4 mg/kg

C.

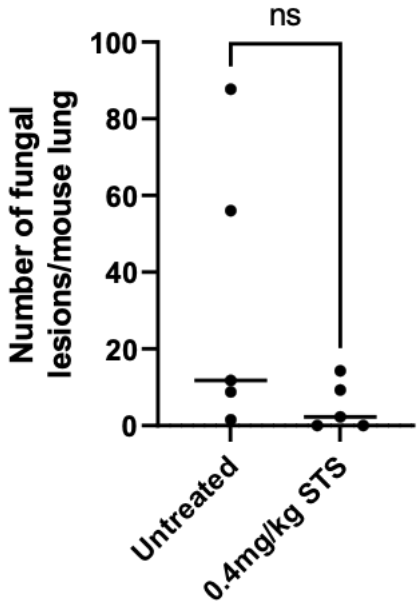
Number of fungal lesions/mouse lung
100
80
60
40
20
0
ns
Untreated
0.4mg/kg STS

D.

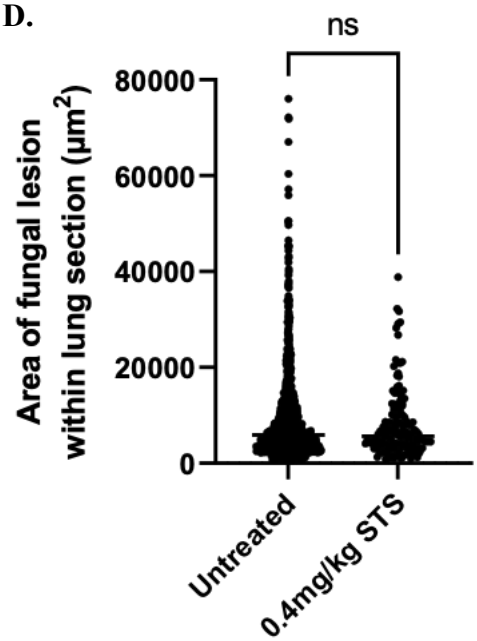
Area of fungal lesion within lung section (μm²)
80000
60000
40000
20000
0
ns
Untreated
0.4mg/kg STS

Figure 4: Staurosporine is significantly protective in mice with invasive aspergillosis

A: Kaplan-Meier curves represent a single independent experiment for STS dose-response experiments in a neutropenic mouse model of invasive pulmonary aspergillosis. Panel shows survival of neutropenic mice intratracheally infected with $5x10^6$ conidia of *A. fumigatus* Af293 and then treated with 0, 0.1, 0.2, or 0.4 mg/kg of STS in 10% DMSO in saline 3h and 48h PI with eight mice per group. A significant difference is indicated (**, $P = 0.0085$) relative to the 10% DMSO in saline group as determined by the Log-rank test.

B: Kaplan-Meir curves present three independent experiments of STS as an antifungal monotherapy in a neutropenic mouse model of invasive pulmonary aspergillosis. Panel shows survival of neutropenic mice intratracheally infected with $5x10^6$ conidia of *A. fumigatus* Af293 and then treated 0.4mg/kg STS administered by IV 3h and 48h PI with eight to ten mice per group. A significant difference is indicated (**, $P = 0.005$) relative to the 10% DMSO in saline-treated group as determined by the Log-rank test.

C-D: The number (C) and area in μm^2 (D) of fungal lesions in GMS-stained pulmonary sections were quantified using QuPath bioimage analysis. Neutropenic mice were infected with $5x10^6$ conidia of *A. fumigatus* Af293, treated with 0 or 0.4mg/kg STS 3h and 24h PI. Their lungs were harvested on day 2 PI for quantitative histology, with five mice per condition, and six sections per lung were taken at 100 μm intervals. The error bars represent the standard deviation. For (C), lesions in each lung section were totalled, with each point representing a mouse and the dash representing the median number of lesions per mouse lung. The significant difference relative to the untreated control was determined by the t-test. For (D), the significant difference relative to the untreated control was determined by the Kolmogorov-Smirnov test.

***A. fumigatus* response to 0.1µg/mL STS for 24h**	**Phosphoproteome**
All phosphopeptides	1,471
Phosphopeptides significantly differentially regulated ($P < 0.05$)	439
Only found in presence of STS	13
Only found in absence of STS	64
Up-phosphorylated with STS	10
Down-phosphorylated with STS	352

Table 1: Summary table of phosphoproteomic analysis by Scaffold 5

Phosphoproteomic results derived from analysis of proteins extracted from *A. fumigatus* Af293 untreated or treated with 0.1µg/mL STS for 24 hours. Five biological replicates were performed and analysed. Analysis of the results was carried out on Scaffold 5. Significant phosphopeptides were sorted based on phosphorylation states in the presence or absence of STS. Significance was determined based on the t-test ($P < 0.05$).

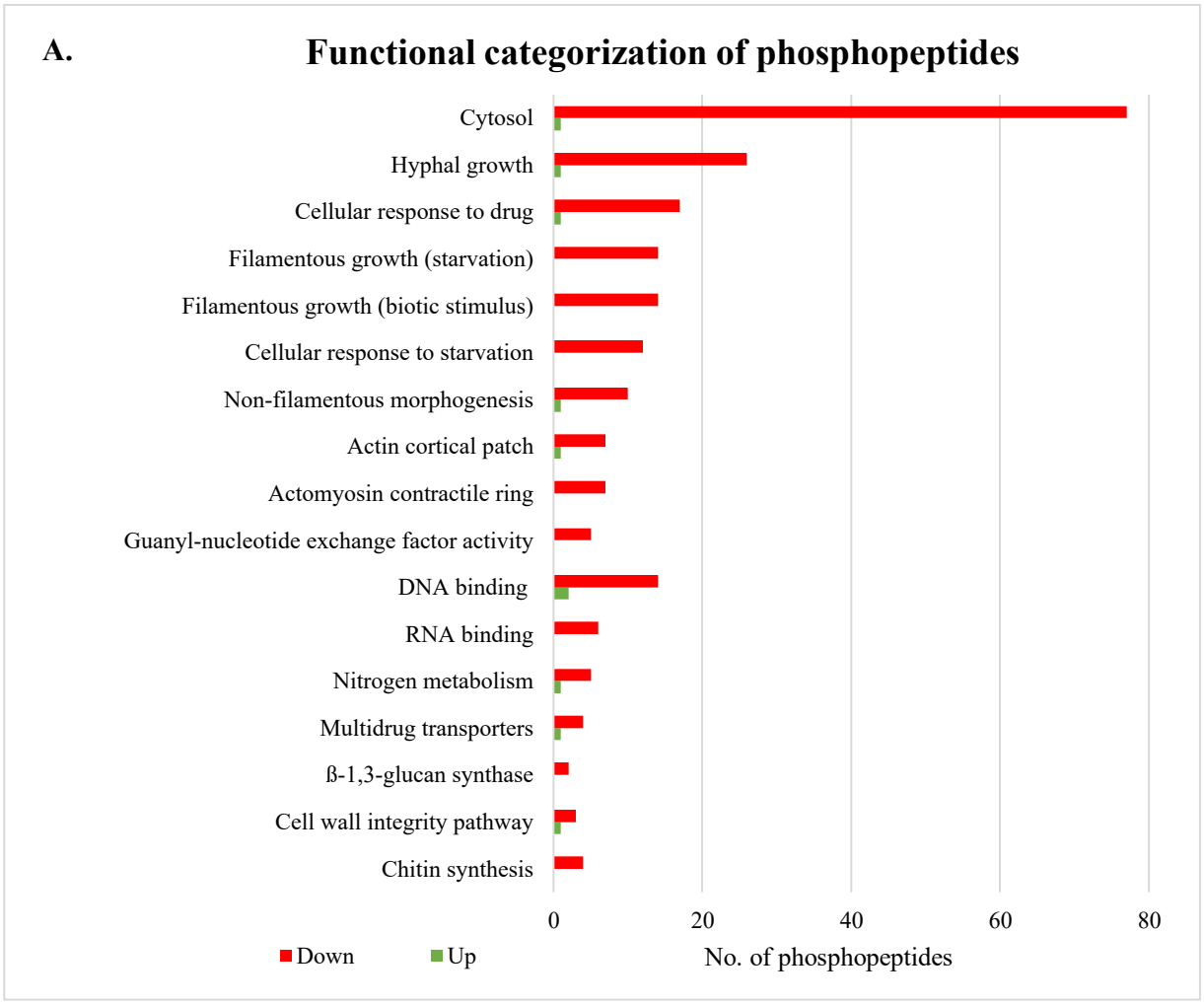
A.
Functional categorization of phosphopeptides
Cytosol
Hyphal growth
Cellular response to drug
Filamentous growth (starvation)
Filamentous growth (biotic stimulus)
Cellular response to starvation
Non-filamentous morphogenesis
Actin cortical patch
Actomyosin contractile ring
Guanyl-nucleotide exchange factor activity
DNA binding
RNA binding
Nitrogen metabolism
Multidrug transporters
ß-1,3-glucan synthase
Cell wall integrity pathway
Chitin synthesis
0
20
40
60
80
Down
Up
No. of phosphopeptides

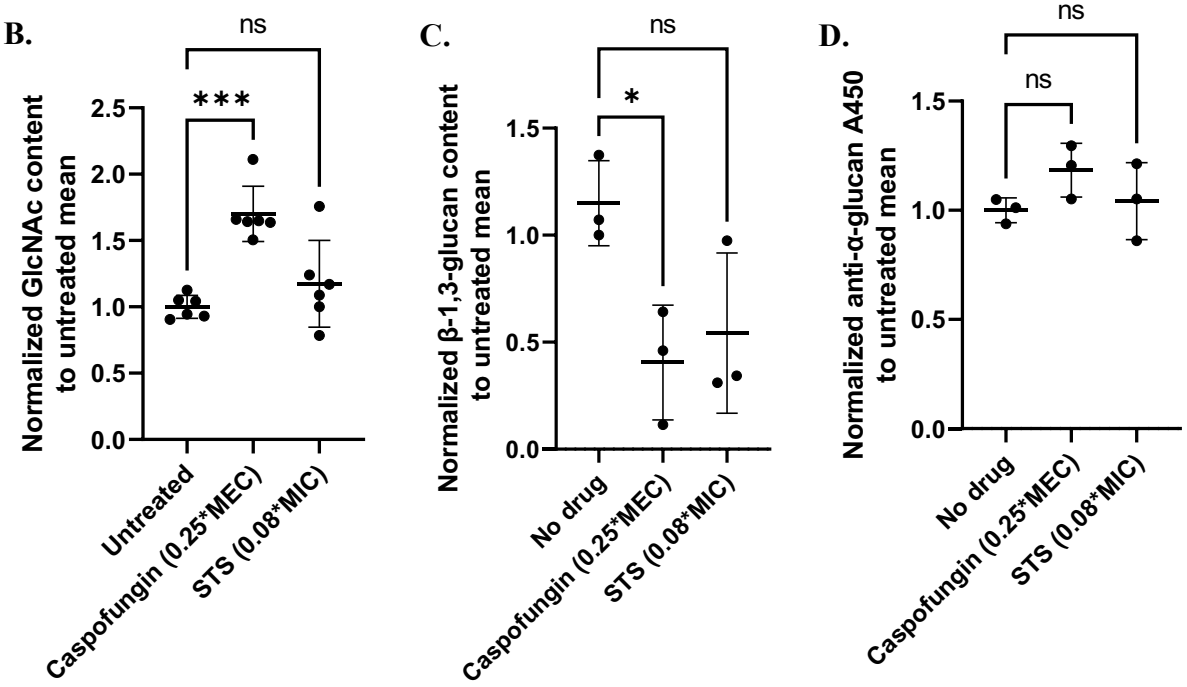
B.
ns
***
Normalized GlcNAc content to untreated mean
2.5
2.0
1.5
1.0
0.5
0.0
Untreated
Caspofungin (0.25*MEC)
STS (0.08*MIC)
C.
ns
*
Normalized β-1,3-glucan content to untreated mean
1.5
1.0
0.5
0.0
No drug
Caspofungin (0.25*MEC)
STS (0.08*MIC)
D.
ns
ns
Normalized anti-α-glucan A450 to untreated mean
1.5
1.0
0.5
0.0
No drug
Caspofungin (0.25*MEC)
STS (0.08*MIC)

Figure 5: Staurosporine exposure in A. fumigatus disables the CWI compensatory pathway and reduces β-(1,3)-D-glucan content in the cell wall.

A: Phosphopeptides significantly differentially phosphorylated upon STS exposure were functionally categorized by FungiFun2 using the GO method. Down-phosphorylated proteins were counted and denoted in red, and up-phosphorylated proteins were counted and denoted in green.

B: GlcNAc content (μmol/mg of cell wall extract mass) was quantified by GC and normalized to the untreated mean (y-axis) for each replicate. Results are two independent experiments, with each experiment testing three replicates of each condition with one point per replicate of the extracted fungal cell wall (x-axis). Error bars represent the standard deviation, and the one-way ANOVA test (***, $P < 0.001$) was performed with comparison to the untreated control.

C: β-(1,3)-D-glucan content (μg/mg of cell wall extract mass) was quantified with the Glucatell assay and then normalized to the untreated mean for each replicate (y-axis). Results are from an experiment performed with three biological replicates of the extracted glucans per experimental condition (x-axis). The error bars represent the standard deviation, and the one-way ANOVA test (*, $P < 0.5$) was performed with comparison to the untreated control.

D: Relative α-glucans content (A450/mg of cell wall extract mass) was quantified by ELISA performed with of anti-α-glucan IgM monoclonal antibody and normalized to the untreated mean of each replicate (y-axis). Results are from an experiment performed with three biological replicates of the extracted glucans per experimental condition (x-axis). Error bars represent the standard deviation, the one-way ANOVA test was performed with comparison to the untreated control.

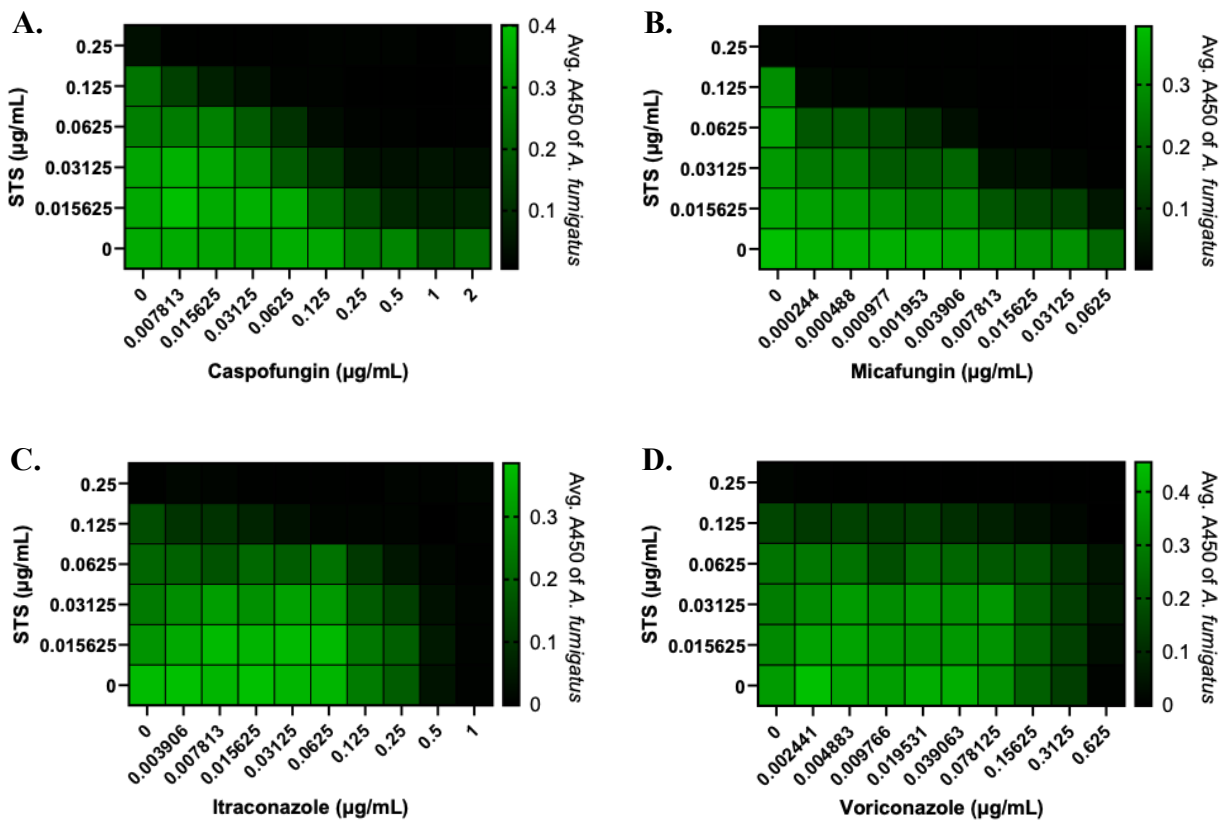

Figure 6: Staurosporine potentiates the activity of echinocandins against A. fumigatus in vitro

A-D: Checkerboard assays were performed using the indicated concentrations of STS (y-axis) in combination with indicated concentrations of echinocandins or azoles against *A. fumigatus* Af293; (A) caspofungin, (B) micafungin, (C) voriconazole, and (D) itraconazole (x-axis). The colour gradient, indicates fungal metabolic activity as quantified by 450nm absorbance using the XTT assay. Panels shown are combined results from three independent experiments.

Fungi	STS + Caspofungin	STS + Micafungin	STS + Itraconazole	STS + Voriconazole
A. fumigatus	√ (S)	√ (S)	x	x
C. albicans	√ (S)	x	√	x
C. auris	√ (S)	√ (S)	-	-
C. glabrata	√ (S)	x	-	-
C. tropicalis	√ (S)	x	-	-
C. parapsilosis	x	x	-	-
C. krusei	x	x	-	-
C. neoformans	x	x	-	-

Table 2: Summary table of checkerboard assays performed with staurosporine

STS was tested in combination with four clinically approved antifungals against a panel of fungal pathogens (N = 3). A '√' represents if potentiation of activity was observed, and 'S' denotes synergy, if the calculated Fractional Inhibitory Concentration Index was below 0.5 at sub-inhibitory concentrations of each agent. An 'x' indicates no potentiation of activity was observed, and a dash indicates the combination was not tested.

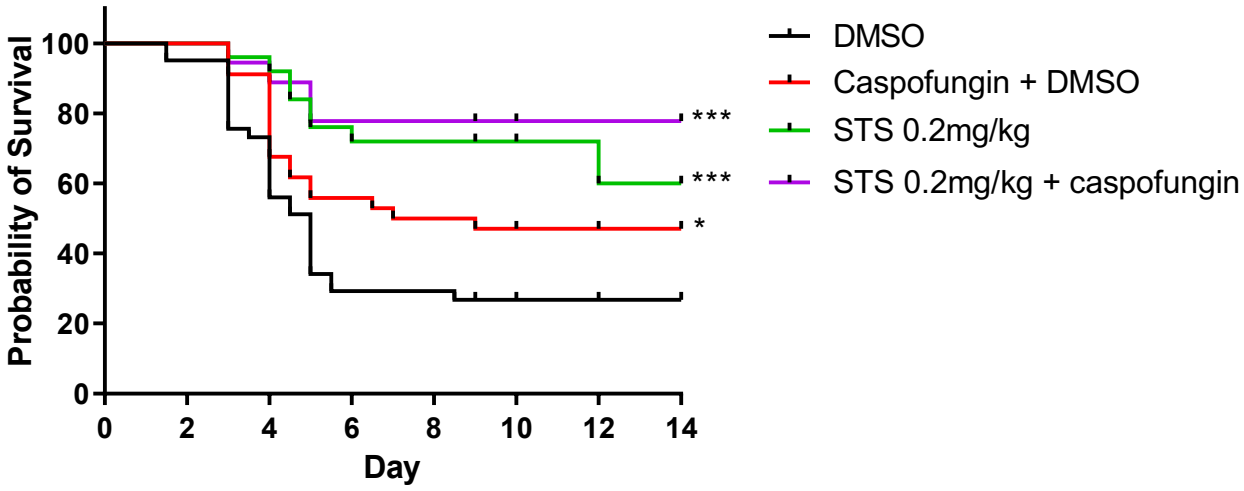

Figure 7: Staurosporine and caspofungin are not synergistic in vivo

Kaplan-Meier curves represent two independent experiments of subtherapeutic STS and caspofungin as a combination therapy in a neutropenic mouse model of invasive pulmonary aspergillosis. Survival of neutropenic mice intratracheally infected with $5x10^6$ conidia of *A. fumigatus* Af293 and then treated with either 0.2 mg/kg of STS in 10% DMSO in saline 3 hours and 48 hours PI, 0.5mg/kg of caspofungin in saline with 10% DMSO 1 hour and every 24 hours PI, or both with 8-10 mice per group. A significant difference is indicated (*, $P < 0.05$) relative to the 10% DMSO in saline-treated group as determined by the Log-rank test. To assess the efficacy of the combination-treated group to the caspofungin- and STS-monotherapy groups, statistical analysis was performed using the Log-rank test.

A.

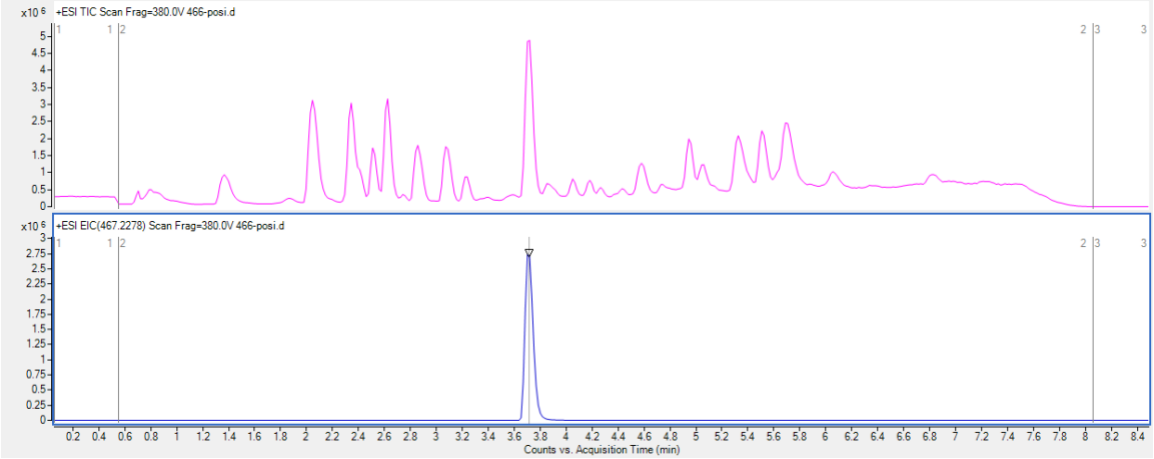

B.

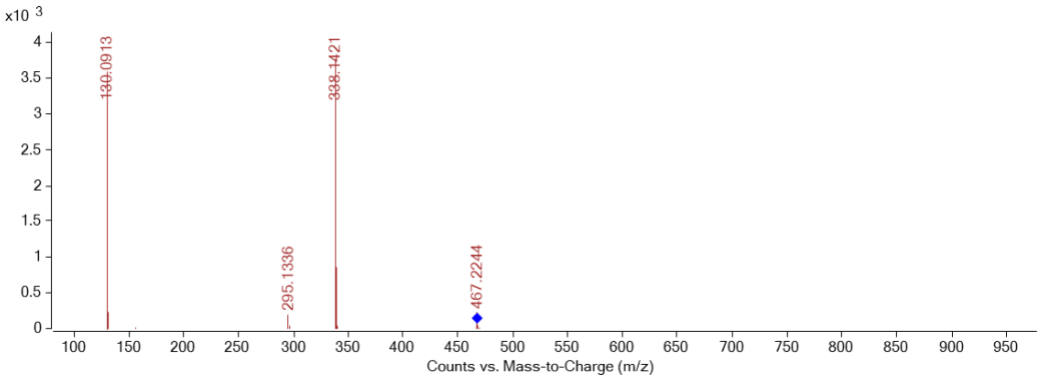

Supplementary Figure 1: An ion at 467m/z found within the semi-purified S. A28 extract fractions which exhibited antifungal activity was identified as staurosporine by MS/MS

A: Liquid chromatography-mass spectrometry (LC-MS) was used to identify the active compound within the elution fraction of the *S. A28* extract with antifungal activity. The graph shows all ions found within the active elution fraction, with the chromatogram with acquisition time on the x-axis and ion intensity on the y-axis to indicate the chromatographic separation of ions. In the top panel, the LC-MS showed the presence of ions found within the active fraction. In the bottom panel, LC-MS identified the most prominent ion in the chromatogram at approximately 3.7 minutes as a [M+H] ion at 467m/z, as the most likely candidate for the antifungal compound.

B: The 467m/z ion identified in panel A was subjected to molecular MS/MS networking, creating ion fragments of the parent molecule. The raw data was inputted into the web-based Global Natural Product Social (GNPS) molecular networking tools, which clustered the data to identify the parent molecule and filtered fragments of the parent molecule within the raw data to create a consensus spectra. This spectrum, shown above, shows a histogram plot of ion fragments of the 467m/z ion on counts vs. mass to charge (x-axis) versus the relative intensity of the ion fragments (y-axis). The fragment mass patterns seen in panel B were matched by the GNPS workflow to that of STS, as determined in previous literature, identifying it as the parent molecule at [M+H] 467 m/z.

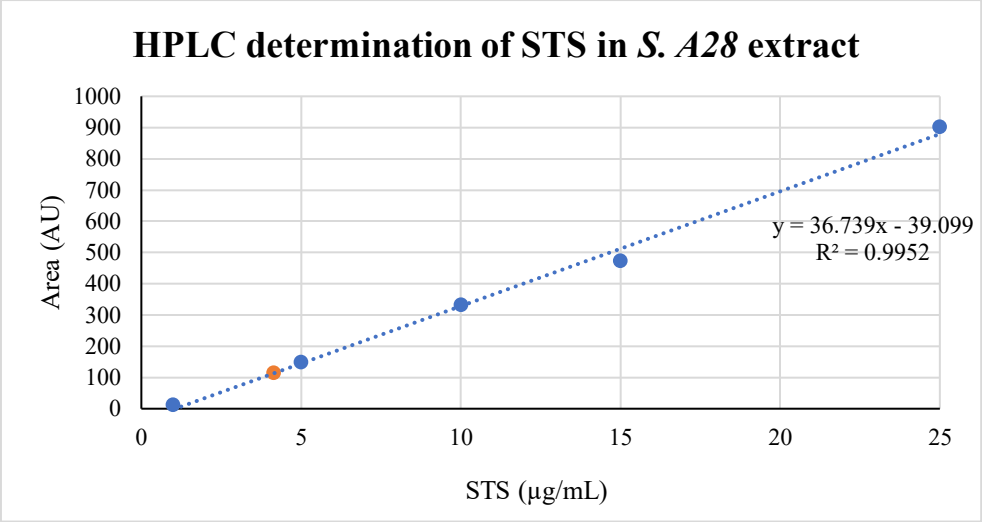

Sample	STS concentration (µg/mL)
1-in-20 dilution of *S. A28* extract (orange)	4.15
Final concentration of STS in *S. A28* extract	83.017

Supplementary Figure 2: HPLC determination of staurosporine concentration in the S. A28 extract

STS (from a stock solution of 5mg/mL in DMSO) was diluted to a range of solutions from 1-25 µg/mL in ddH_2O. These solutions were analysed by HPLC coupled to UV-Vis spectroscopy at 292 nm and used to generate a standard curve based on STS concentration to the area under the peak of the HPLC-generated chromatogram tracking time over 292nm absorbance (points in blue). Solutions with solely DMSO at the same proportion as the STS solutions were also analysed to verify signals seen at 292nm were not due to DMSO. A 1-in-20 dilution of an *S. A28* extract was assayed by HPLC using the same method to determine the concentration of STS using the standard curve (shown in the orange point).

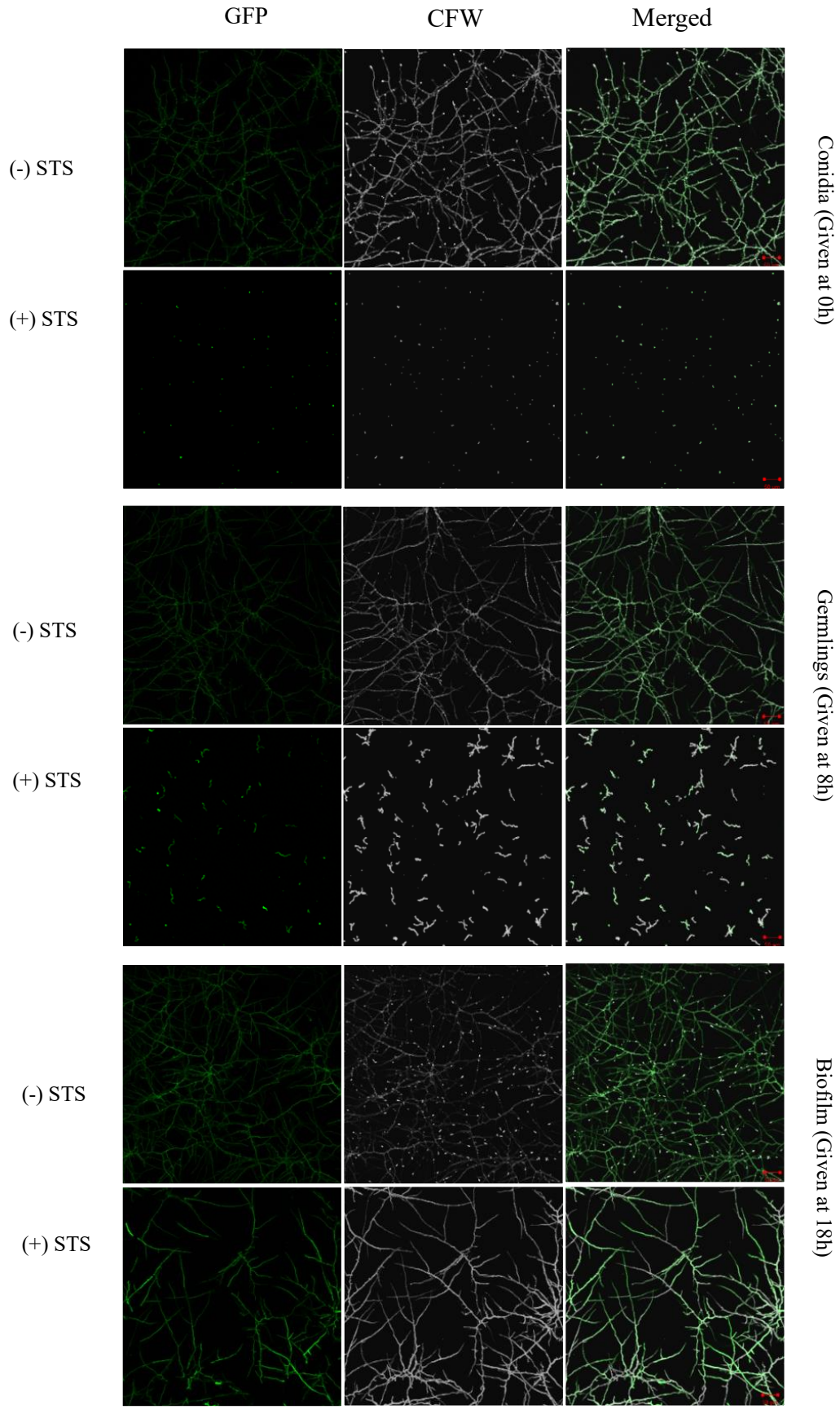
GFP
CFW
Merged
(-) STS
(+) STS
Conidia (Given at 0h)
(-) STS
(+) STS
Germlings (Given at 8h)
(-) STS
(+) STS
Biofilm (Given at 18h)

Supplementary Figure 3: Staurosporine exhibits fungicidal antifungal against A. fumigatus that is most marked in conidia and young hyphae

GFP-expressing *A. fumigatus* Af293 strain (green) was grown in RPMI 1640 The growth stages tested included dormant conidia (0h growth), young germlings (8h growth), and hyphal biofilm (18 h growth). Samples were then further grown for 16h at 37˚C in 5% CO_2 with or without 0.1 µg/mL of STS. Organisms were counterstained with a 1 in 400 dilution of CFW before confocal microscopy analysis at an objective of 20X. Images show single-stain GFP, CFW, and merged (from left to right) from a single replicate of an experiment performed in triplicate.

Footnotes

Funding

This project was supported by the McGill University Health Center Student Fellowship Award to E.J. Côté and a CIHR Foundation Award FDN159902 to D. C. Sheppard.

Acknowledgments

We would like to acknowledge the Molecular Imaging, Histopathology, Proteomics and Molecular Analysis platforms at the McGill University Health Centre Research Institute for their services and contribution to this work.

Conflicts of interest

The authors of this work have no conflicts of interest to report. Parts of this work have been presented at the 7th Infectious Diseases and Immunity in Global Health Research Day, Montreal QC. May 5th, 2023, Advances Against Aspergillosis and Mucormycosis, online, February 2-3rd

2022 and in Milan, Italy Jan. 25-27th 2024, and the 11th Trends in Medical Mycology conference, Athens, Greece, Oct. 20-23rd 2023.

Chapter 3: General discussion and conclusions

In this work, we discovered that a natural product from an Arctic *Streptomyces*, STS, has a broad range of antifungal activity against fungi, including human fungal pathogens. We further demonstrated that STS has significant activity *in vivo*, it is an effective monotherapy to treat invasive aspergillosis in mice and may synergize with the echinocandin class of antifungals. We have begun to elucidate a mechanism of action of STS involving several cell wall glycan synthases and compensatory pathways associated with cell wall stress.

STS was as potent or more so than amphotericin B against multiple human fungal pathogens, including all pathogens belonging to the critical group on the WHO fungal priority pathogen list and several from the high priority group (93, 94). STS exhibited significant antifungal activity against invasive aspergillosis in mice at 0.4mg/kg. STS has been previously tested in mice as an anti-tumour treatment, at doses of 0.8mg/kg, after which the researchers did see a decline in body weight (141). The tolerability study we performed did not show a decline in body weight with 0.8mg/kg of STS, but the mice had displayed clear signs of anxiety and distress. We further demonstrated that therapy with STS at 0.2mg/kg still results in a 60% survival rate in *A. fumigatus*-infected mice. Despite these findings, it will likely be challenging to continue the development of STS as an antifungal in light of the extensive data on its cytotoxicity and its common use in the lab as an agent for the induction of apoptosis (134).

One approach to improve the tolerability of STS could be the investigation of novel delivery formulations. In studies of STS as an anti-cancer treatment, the effect of free versus liposome-encapsulated STS was evaluated. Liposomal STS was shown to tend to accumulate more in the tumours compared to free-form STS, and the mice treated with liposomal STS had no symptoms of toxicity (141). Liposomes have higher cellular affinity and better tissue compatibility compared

to free drugs, using encapsulated STS could therefore potentially reduce the cytotoxicity of this agent during therapy of fungal infection (156). Liposome encapsulation of the antifungal amphotericin B has been highly successful in reducing toxicity while retaining efficacy, with this formulation now in common clinical use (59, 157). Liposomes themselves are unspecific but can be modified to specifically target fungi (158). Antifungals encapsulated in liposomes decorated with dectins, called DectiSomes, have been found to be more effective as antifungals *in vitro* and *in vivo* than their untargeted forms; the dectin-coating targets the liposome towards the fungal cell wall and exopolysaccharide matrices (158, 159). Encapsulation of STS by DectiSomes could also improve its efficacy and toxicity both *in vitro* and *in vivo* (160).

Beyond our studies of the efficacy of STS as an antifungal agent, we performed initial studies to probe the mechanism by which this agent inhibits *A. fumigatus* growth. We found that STS exposure results in the reduced phosphorylation of multiple cell wall glycan synthases, including Fks1. The phosphorylation sites were found within the accessory domain of the Fks1 enzyme. Although the effect of phosphorylation of these sites has not been studied, mutations in this region are associated with changes in the structure of the catalytic domain and reduced enzyme function (144). Down-phosphorylation of this domain could potentially result in a similar structural change, and thereby reducing function. This hypothesis is consistent with the trend to lower β-(1,3)-D-glucan levels measured in the cell wall extract of STS treated-*A. fumigatus*. The observed synergy with echinocandins could also reflect this effect on Fks1 activity and lower β-(1,3)-D-glucan levels as both agents impact the same fungal cell wall pathway. Studies to investigate the synergy of these agents were not conclusive and may reflect a need to test lower concentrations of STS or differences in pharmacodynamics or microenvironmental conditions *in vivo.* Further studies are required to define if echinocandin-STS synergy occurs *in vivo*. As synergy between STS and

micafungin had also been observed against *A. fumigatus in vitro*, it may also be prudent to investigate if they synergize *in vivo* within an invasive aspergillosis model.

Although the phosphoproteomic data provide a potential mechanism of action for STS, it will be challenging to definitively identify the specific antifungal mechanism of STS in *A. fumigatus.* STS inhibits multiple target kinases, likely resulting in multiple effects that may contribute to the fungicidal activity of STS. Beyond cell wall glycan synthases and the CWI pathway, several proteins involved in nitrogen metabolism also exhibited altered phosphorylation patterns. GATA transcription factors AreA and AreaB, which regulate the expression of nitrogen metabolism genes, and the ammonium transporter MeaA were down-phosphorylated with STS exposure (161). The nitrate transporter NrtB is only found phosphorylated in the presence of STS, yet the nitrate reductase NiiA was only phosphorylated in the absence of STS (161, 162). The impact of STS on sensing, regulation, and detoxification of nitrogen could be explored through culturing STS-exposed *A. fumigatus* on media containing different sources of nitrogen. Nitrogen metabolism is just one of many effects of STS that were observed in the phosphoproteomic results, showing the broad activity of STS within *A. fumigatus*. Prior studies have shown STS induces programmed cell death in multiple human cell lines and even in the filamentous fungus *Neurospora crassa*, yet we did not identify any programmed cell death-associated proteins of *A. fumigatus* in the phosphoproteomic analysis results (163-167). Although a challenging task, the identification of the relevant targets within *A. fumigatus* could inform efforts to reduce the toxicity of STS. With these targets, structure-based optimization could be used to synthesize a fungal-specific inhibitor and the reduction of host cell toxicity.

One of the main findings from the project is the possibility that STS down-phosphorylates Fks1 in *A. fumigatus*, resulting in a decrease of β-(1,3)-D-glucan content in the cell wall.

Echinocandin resistance in *Aspergillus* is rare, but a few clinical cases have been reported (84, 91). Mechanisms of resistance include hotspot mutations in the Fks1 catalytic subunit, lower binding affinity of echinocandin to the Fks1 enzyme, and changes in the lipid microenvironment around the enzyme that impact drug access to the target (84, 98, 168). A future direction could be to test if the STS is still effective in these resistant *A. fumigatus* strains, and if the impact on β-(1,3)-D-glucan levels would remain the same.

This project mainly focused on the activity of STS against *A. fumigatus*, as it was the most susceptible pathogen to STS monotherapy and combination therapy with caspofungin or micafungin. The activity of STS against other fungal pathogens, such as the *Candida* species, was much more variable. For example, *C. auris* was the fungal pathogen with the highest STS IC_{50}, indicating this pathogen may be inherently more resistant to STS. Phosphoproteomic analysis of STS-treated *C. auris* could provide further information regarding the identity of a significant target in *Candida*. It has been previously shown that deletion of the *C. albicans* homolog of protein kinase C, Pkc1, attenuates *C. albicans* virulence in a murine model of systemic candidiasis (149). Based on the finding of PkcA down-phosphorylation by STS in *A. fumigatus*, treatment with STS could have a similar effect in *C. albicans* and other *Candida* species.

Although we found the active antifungal agent produced by *S. A28* was not a novel molecule, our studies have advanced our understanding of the antifungal potential of STS. There is an urgent need to identify novel agents to expand the antifungal arsenal (4). Invasive fungal diseases are a serious threat to human health, with more than 6 million people becoming severely ill and 3 million deaths annually (2). These numbers are expected to increase, in part as a consequence of the rise of antifungal resistance (4, 169). The most traditional method of novel antifungal discovery is natural product screening for secondary metabolites with antimicrobial activity produced by

microorganisms from diverse natural environments (106). A modern method currently employed by many researchers worldwide is to bioprospect unique and poorly characterized microbiomes, such as the Arctic, to limit the chance of re-isolating previously discovered natural products (111). The work in this project demonstrates this approach still carries the risk of rediscovery of known molecules. Even though *S. A28* was confirmed as a novel species, *Streptomyces* are well-known sources of antimicrobials and have been heavily characterized, and our work eventually led to the re-identification of a known compound (170). Instead of focusing on novel species of known genera, it may be more effective to focus on novel genera and their natural products. This approach, however, is limited by the fact only a fraction of microorganisms can be cultured under laboratory conditions, especially those from extreme environments like the Arctic. Techniques such as metagenomics, cell sorting, and single-cell sequencing have been used to address this limitation (171).

Overall, this project demonstrates how even previously described molecules can hold antifungal potential. Further functional analysis and medicinal chemistry may be helpful to develop more specific and safer derivatives of STS that retain antifungal activity and exhibit reduced host cell toxicity. Our studies of STS open the door to the investigation of kinase inhibitors as antifungal agents, which may contribute towards mitigating the crisis of a shrinking arsenal of therapies for the treatment of fungal diseases (2, 4).

References:

1. Kainz K, Bauer MA, Madeo F, Carmona-Gutierrez D. 2020. Fungal infections in humans: the silent crisis. Microbial Cell 7:143-145.
2. Denning DW. 2024. Global incidence and mortality of severe fungal disease. The Lancet Infectious Diseases doi:https://doi.org/10.1016/S1473-3099(23)00692-8.
3. Rodrigues ML, Nosanchuk JD. 2020. Fungal diseases as neglected pathogens: A wake-up call to public health officials. PLOS Neglected Tropical Diseases 14:e0007964.
4. Denning DW, Bromley MJ. 2015. How to bolster the antifungal pipeline. Science 347:1414-1416.
5. Hokken MWJ, Zwaan BJ, Melchers WJG, Verweij PE. 2019. Facilitators of adaptation and antifungal resistance mechanisms in clinically relevant fungi. Fungal Genetics and Biology 132:103254.
6. Ben-Ami R, Berman J, Novikov A, Bash E, Shachor-Meyouhas Y, Zakin S, Maor Y, Tarabia J, Schechner V, Adler A, Finn T. 2017. Multidrug-Resistant Candida haemulonii and C. auris, Tel Aviv, Israel. Emerging infectious diseases 23:195-203.
7. Posch W, Blatzer M, Wilflingseder D, Lass-Flörl C. 2018. Aspergillus terreus: Novel lessons learned on amphotericin B resistance. Medical Mycology 56:S73-S82.
8. Taylor LH, Latham SM, Woolhouse ME. 2001. Risk factors for human disease emergence. Philos Trans R Soc Lond B Biol Sci 356:983-9.
9. Bongomin F, Gago S, Oladele RO, Denning DW. 2017. Global and Multi-National Prevalence of Fungal Diseases-Estimate Precision. Journal of fungi (Basel, Switzerland) 3:57.

10. Brown GD, Denning DW, Gow NAR, Levitz SM, Netea MG, White TC. 2012. Hidden Killers: Human Fungal Infections. Science Translational Medicine 4:165rv13-165rv13.
11. Vallabhaneni S, Mody RK, Walker T, Chiller T. 2016. The Global Burden of Fungal Diseases. Infectious Disease Clinics of North America 30:1-11.
12. Low CY, Rotstein C. 2011. Emerging fungal infections in immunocompromised patients. F1000 Med Rep 3:14.
13. Mei-Sheng Riley M. 2021. Invasive Fungal Infections Among Immunocompromised Patients in Critical Care Settings: Infection Prevention Risk Mitigation. Critical Care Nursing Clinics of North America 33:395-405.
14. Rogers TR. 1995. Epidemiology and control of nosocomial fungal infections. Current Opinion in Infectious Diseases 8.
15. Denning DW. 1998. Invasive Aspergillosis. Clinical Infectious Diseases 26:781-803.
16. Denning DW, Hope WW. 2010. Therapy for fungal diseases: opportunities and priorities. Trends Microbiol 18:195-204.
17. Garcia-Solache MA, Casadevall A. 2010. Global warming will bring new fungal diseases for mammals. mBio 1:e00061-10.
18. Gorris ME, Treseder KK, Zender CS, Randerson JT. 2019. Expansion of Coccidioidomycosis Endemic Regions in the United States in Response to Climate Change. Geohealth 3:308-327.
19. Benedict K, Park BJ. 2014. Invasive Fungal Infections after Natural Disasters. Emerging Infectious Disease Journal 20:349-355.
20. Casadevall A. 2012. Fungi and the Rise of Mammals. PLOS Pathogens 8:e1002808.

21. Gugnani HC. 2003. Ecology and taxonomy of pathogenic aspergilli. Front Biosci 8:s346-57.

22. Dagenais TR, Keller NP. 2009. Pathogenesis of Aspergillus fumigatus in Invasive Aspergillosis. Clin Microbiol Rev 22:447-65.

23. Latgé JP. 1999. Aspergillus fumigatus and aspergillosis. Clin Microbiol Rev 12:310-50.

24. Tekaia F, Latgé J-P. 2005. Aspergillus fumigatus: saprophyte or pathogen? Current Opinion in Microbiology 8:385-392.

25. Latgé JP, Chamilos G. 2019. Aspergillus fumigatus and Aspergillosis in 2019. Clin Microbiol Rev 33.

26. van de Veerdonk FL, Gresnigt MS, Romani L, Netea MG, Latgé J-P. 2017. Aspergillus fumigatus morphology and dynamic host interactions. Nature Reviews Microbiology 15:661-674.

27. Le Mauff F. 2020. Exopolysaccharides and Biofilms, p 225-254. *In* Latgé J-P (ed), The Fungal Cell Wall : An Armour and a Weapon for Human Fungal Pathogens doi:10.1007/82_2020_199. Springer International Publishing, Cham.

28. Bowman SM, Free SJ. 2006. The structure and synthesis of the fungal cell wall. Bioessays 28:799-808.

29. Latgé J-P. 2023. Cell wall of Aspergillus fumigatus: Variability and response to stress. Fungal Biology doi:https://doi.org/10.1016/j.funbio.2023.05.001.

30. Valsecchi I, Dupres V, Michel JP, Duchateau M, Matondo M, Chamilos G, Saveanu C, Guijarro JI, Aimanianda V, Lafont F. 2019. The puzzling construction of the conidial outer layer of Aspergillus fumigatus. Cellular microbiology 21:e12994.

31. Aimanianda V, Bayry J, Bozza S, Kniemeyer O, Perruccio K, Elluru SR, Clavaud C, Paris S, Brakhage AA, Kaveri SV. 2009. Surface hydrophobin prevents immune recognition of airborne fungal spores. Nature 460:1117-1121.

32. Latgé J-P, Beauvais A, Chamilos G. 2017. The Cell Wall of the Human Fungal Pathogen Aspergillus fumigatus: Biosynthesis, Organization, Immune Response, and Virulence. Annual Review of Microbiology 71:99-116.

33. Chakraborty A, Fernando LD, Fang W, Dickwella Widanage MC, Wei P, Jin C, Fontaine T, Latgé J-P, Wang T. 2021. A molecular vision of fungal cell wall organization by functional genomics and solid-state NMR. Nature Communications 12:6346.

34. Sheppard DC. 2011. Molecular mechanism of Aspergillus fumigatus adherence to host constituents. Curr Opin Microbiol 14:375-9.

35. Hillmann F, Novohradská S, Mattern DJ, Forberger T, Heinekamp T, Westermann M, Winckler T, Brakhage AA. 2015. Virulence determinants of the human pathogenic fungus Aspergillus fumigatus protect against soil amoeba predation. Environ Microbiol 17:2858-69.

36. Orciuolo E, Stanzani M, Canestraro M, Galimberti S, Carulli G, Lewis R, Petrini M, Komanduri KV. 2007. Effects of Aspergillus fumigatus gliotoxin and methylprednisolone on human neutrophils: implications for the pathogenesis of invasive aspergillosis. J Leukoc Biol 82:839-48.

37. Schlam D, Canton J, Carreño M, Kopinski H, Freeman SA, Grinstein S, Fairn GD. 2016. Gliotoxin Suppresses Macrophage Immune Function by Subverting Phosphatidylinositol 3,4,5-Trisphosphate Homeostasis. mBio 7:e02242.

38. Kamei K, Watanabe A. 2005. Aspergillus mycotoxins and their effect on the host. Medical Mycology 43:S95-S99.

39. Kogan TV, Jadoun J, Mittelman L, Hirschberg K, Osherov N. 2004. Involvement of Secreted Aspergillus fumigatus Proteases in Disruption of the Actin Fiber Cytoskeleton and Loss of Focal Adhesion Sites in Infected A549 Lung Pneumocytes. The Journal of Infectious Diseases 189:1965-1973.

40. Matthaiou EI, Sass G, Stevens DA, Hsu JL. 2018. Iron: an essential nutrient for Aspergillus fumigatus and a fulcrum for pathogenesis. Curr Opin Infect Dis 31:506-511.

41. Chrdle A, Mustakim S, Bright-Thomas RJ, Baxter CG, Felton T, Denning DW. 2012. Aspergillus bronchitis without significant immunocompromise. Ann N Y Acad Sci 1272:73-85.

42. Denning D, Pleuvry A, Cole D. 2010. Global burden of ABPA in adults with asthma and its complication chronic pulmonary aspergillosis. Manuscript submitted.

43. Prigitano A, Esposto MC, Biffi A, De Lorenzis G, Favuzzi V, Koncan R, Lo Cascio G, Barao Ocampo M, Colombo C, Pizzamiglio G, Romanò L, Tortorano AM. 2017. Triazole resistance in Aspergillus fumigatus isolates from patients with cystic fibrosis in Italy. Journal of Cystic Fibrosis 16:64-69.

44. Malhotra S, Sharma S, Bhatia N, Kumar P, Bhatia N, Patil V, Hans C. 2014. Recent diagnostic techniques in mycology. Journal of Medical Microbiology & Diagnosis 3:1.

45. AlMaghrabi RS, Al-Musawi T, Albaksami O, Subhi AL, Fakih RE, Stone NR. 2023. Challenges in the Management of Invasive Fungal Infections in the Middle East: Expert Opinion to Optimize Management Using a Multidisciplinary Approach. Cureus 15:e44356.

46. Delma FZ, Al-Hatmi AMS, Brüggemann RJM, Melchers WJG, de Hoog S, Verweij PE, Buil JB. 2021. Molecular Mechanisms of 5-Fluorocytosine Resistance in Yeasts and Filamentous Fungi. J Fungi (Basel) 7.

47. Vermes A, Guchelaar H-J, Dankert J. 2000. Flucytosine: a review of its pharmacology, clinical indications, pharmacokinetics, toxicity and drug interactions. Journal of Antimicrobial Chemotherapy 46:171-179.

48. Nett JE, Andes DR. 2016. Antifungal Agents: Spectrum of Activity, Pharmacology, and Clinical Indications. Infectious Disease Clinics of North America 30:51-83.

49. Sastré-Velásquez LE, Dallemulle A, Kühbacher A, Baldin C, Alcazar-Fuoli L, Niedrig A, Müller C, Gsaller F. 2022. The fungal expel of 5-fluorocytosine derived fluoropyrimidines mitigates its antifungal activity and generates a cytotoxic environment. PLoS Pathog 18:e1011066.

50. Verweij PE, Te Dorsthorst DT, Janssen WH, Meis JF, Mouton JW. 2008. In vitro activities at pH 5.0 and pH 7.0 and in vivo efficacy of flucytosine against Aspergillus fumigatus. Antimicrob Agents Chemother 52:4483-5.

51. Ullmann AJ, Aguado JM, Arikan-Akdagli S, Denning DW, Groll AH, Lagrou K, Lass-Flörl C, Lewis RE, Munoz P, Verweij PE, Warris A, Ader F, Akova M, Arendrup MC, Barnes RA, Beigelman-Aubry C, Blot S, Bouza E, Brüggemann RJM, Buchheidt D, Cadranel J, Castagnola E, Chakrabarti A, Cuenca-Estrella M, Dimopoulos G, Fortun J, Gangneux JP, Garbino J, Heinz WJ, Herbrecht R, Heussel CP, Kibbler CC, Klimko N, Kullberg BJ, Lange C, Lehrnbecher T, Löffler J, Lortholary O, Maertens J, Marchetti O, Meis JF, Pagano L, Ribaud P, Richardson M, Roilides E, Ruhnke M, Sanguinetti M, Sheppard DC, Sinkó J, Skiada A, et al. 2018. Diagnosis and management of Aspergillus

diseases: executive summary of the 2017 ESCMID-ECMM-ERS guideline. Clinical Microbiology and Infection 24:e1-e38.

52. Kathiravan MK, Salake AB, Chothe AS, Dudhe PB, Watode RP, Mukta MS, Gadhwe S. 2012. The biology and chemistry of antifungal agents: A review. Bioorganic & Medicinal Chemistry 20:5678-5698.

53. Maertens JA. 2004. History of the development of azole derivatives. Clinical Microbiology and Infection 10:1-10.

54. Ashu EE, Korfanty GA, Samarasinghe H, Pum N, You M, Yamamura D, Xu J. 2018. Widespread amphotericin B-resistant strains of Aspergillus fumigatus in Hamilton, Canada. Infect Drug Resist 11:1549-1555.

55. Park N-H, Shin K-H, Kang MK. 2017. 34 - Antifungal and Antiviral Agents, p 488-503. *In* Dowd FJ, Johnson BS, Mariotti AJ (ed), Pharmacology and Therapeutics for Dentistry (Seventh Edition) doi:https://doi.org/10.1016/B978-0-323-39307-2.00034-5. Mosby.

56. Di Mambro T, Guerriero I, Aurisicchio L, Magnani M, Marra E. 2019. The Yin and Yang of Current Antifungal Therapeutic Strategies: How Can We Harness Our Natural Defenses? Frontiers in Pharmacology 10.

57. Anderson TM, Clay MC, Cioffi AG, Diaz KA, Hisao GS, Tuttle MD, Nieuwkoop AJ, Comellas G, Maryum N, Wang S, Uno BE, Wildeman EL, Gonen T, Rienstra CM, Burke MD. 2014. Amphotericin forms an extramembranous and fungicidal sterol sponge. Nat Chem Biol 10:400-6.

58. Haro-Reyes T, Díaz-Peralta L, Galván-Hernández A, Rodríguez-López A, Rodríguez-Fragoso L, Ortega-Blake I. 2022. Polyene Antibiotics Physical Chemistry and Their

Effect on Lipid Membranes; Impacting Biological Processes and Medical Applications. Membranes (Basel) 12.

59. Olson JA, Schwartz JA, Hahka D, Nguyen N, Bunch T, Jensen GM, Adler-Moore JP. 2014. Toxicity and efficacy differences between liposomal amphotericin B formulations in uninfected and Aspergillus fumigatus infected mice. Medical Mycology 53:107-118.

60. Maxfield L, Preuss CV, Bermudez R. 2022. Terbinafine, StatPearls. StatPearls Publishing Copyright © 2022, StatPearls Publishing LLC., Treasure Island (FL).

61. Gupta AK, Ryder JE, Chow M, Cooper EA. 2005. Dermatophytosis: the management of fungal infections. Skinmed 4:305-10.

62. Sucher AJ, Chahine EB, Balcer HE. 2009. Echinocandins: the newest class of antifungals. Ann Pharmacother 43:1647-57.

63. Grover ND. 2010. Echinocandins: A ray of hope in antifungal drug therapy. Indian journal of pharmacology 42:9-11.

64. Perlin DS. 2011. Current perspectives on echinocandin class drugs. Future Microbiol 6:441-57.

65. Walker LA, Lee KK, Munro CA, Gow NA. 2015. Caspofungin Treatment of Aspergillus fumigatus Results in ChsG-Dependent Upregulation of Chitin Synthesis and the Formation of Chitin-Rich Microcolonies. Antimicrob Agents Chemother 59:5932-41.

66. Dichtl K, Samantaray S, Wagener J. 2016. Cell wall integrity signalling in human pathogenic fungi. Cellular Microbiology 18:1228-1238.

67. Dockrell DH. 2008. Salvage therapy for invasive aspergillosis. Journal of Antimicrobial Chemotherapy 61:i41-i44.

68. Campitelli M, Zeineddine N, Samaha G, Maslak S. 2017. Combination Antifungal Therapy: A Review of Current Data. J Clin Med Res 9:451-456.

69. Roilides E, Iosifidis E. 2019. Acquired resistance in fungi: how large is the problem? Clinical Microbiology and Infection 25:790-791.

70. Weinbergerova B, Kocmanova I, Racil Z, Mayer J. 2017. Serological Approaches, p 209-221. *In* Lion T (ed), Human Fungal Pathogen Identification: Methods and Protocols doi:10.1007/978-1-4939-6515-1_11. Springer New York, New York, NY.

71. Dichtl K, Helmschrott C, Dirr F, Wagener J. 2012. Deciphering cell wall integrity signalling in Aspergillus fumigatus: identification and functional characterization of cell wall stress sensors and relevant Rho GTPases. Molecular Microbiology 83:506-519.

72. Rocha MC, Fabri JH, Franco de Godoy K, Alves de Castro P, Hori JI, Ferreira da Cunha A, Arentshorst M, Ram AF, van den Hondel CA, Goldman GH, Malavazi I. 2016. Aspergillus fumigatus MADS-Box Transcription Factor rlmA Is Required for Regulation of the Cell Wall Integrity and Virulence. G3 (Bethesda) 6:2983-3002.

73. Malavazi I, Goldman GH, Brown NA. 2014. The importance of connections between the cell wall integrity pathway and the unfolded protein response in filamentous fungi. Brief Funct Genomics 13:456-70.

74. Leonardelli F, Macedo D, Dudiuk C, Cabeza MS, Gamarra S, Garcia-Effron G. 2016. Aspergillus fumigatus Intrinsic Fluconazole Resistance Is Due to the Naturally Occurring T301I Substitution in Cyp51Ap. Antimicrob Agents Chemother 60:5420-6.

75. Arendrup MC, Perlin DS. 2014. Echinocandin resistance: an emerging clinical problem? Current opinion in infectious diseases 27:484-492.

76. Snelders E, Melchers WJ, Verweij PE. 2011. Azole resistance in Aspergillus fumigatus: a new challenge in the management of invasive aspergillosis? Future Microbiology 6:335-347.

77. Cannon Richard D, Lamping E, Holmes Ann R, Niimi K, Baret Philippe V, Keniya Mikhail V, Tanabe K, Niimi M, Goffeau A, Monk Brian C. 2009. Efflux-Mediated Antifungal Drug Resistance. Clinical Microbiology Reviews 22:291-321.

78. Lee Y, Robbins N, Cowen LE. 2023. Molecular mechanisms governing antifungal drug resistance. npj Antimicrobials and Resistance 1:5.

79. Sen P, Vijay M, Kamboj H, Gupta L, Shankar J, Vijayaraghavan P. 2024. cyp51A mutations, protein modeling, and efflux pump gene expression reveals multifactorial complexity towards understanding Aspergillus section Nigri azole resistance mechanism. Scientific Reports 14:6156.

80. Morio F, Loge C, Besse B, Hennequin C, Le Pape P. 2010. Screening for amino acid substitutions in the Candida albicans Erg11 protein of azole-susceptible and azole-resistant clinical isolates: new substitutions and a review of the literature. Diagnostic Microbiology and Infectious Disease 66:373-384.

81. Marichal P, Koymans L, Willemsens S, Bellens D, Verhasselt P, Luyten W, Borgers M, Ramaekers FCS, Odds FC, Vanden Bossche H. 1999. Contribution of mutations in the cytochrome P450 14α-demethylase (Erg11p, Cyp51p) to azole resistance in Candida albicans. Microbiology 145:2701-2713.

82. Pérez-Cantero A, López-Fernández L, Guarro J, Capilla J. 2020. Azole resistance mechanisms in Aspergillus: update and recent advances. International Journal of Antimicrobial Agents 55:105807.

83. Dick JD, Merz WG, Saral R. 1980. Incidence of polyene-resistant yeasts recovered from clinical specimens. Antimicrobial Agents and Chemotherapy 18:158-163.

84. Jiménez-Ortigosa C, Moore C, Denning David W, Perlin David S. 2017. Emergence of Echinocandin Resistance Due to a Point Mutation in the fks1 Gene of Aspergillus fumigatus in a Patient with Chronic Pulmonary Aspergillosis. Antimicrobial Agents and Chemotherapy 61:10.1128/aac.01277-17.

85. Garcia-Effron G, Lee S, Park S, Cleary JD, Perlin DS. 2009. Effect of Candida glabrata FKS1 and FKS2 mutations on echinocandin sensitivity and kinetics of 1,3-beta-D-glucan synthase: implication for the existing susceptibility breakpoint. Antimicrob Agents Chemother 53:3690-9.

86. Castanheira M, Woosley LN, Diekema DJ, Messer SA, Jones RN, Pfaller MA. 2010. Low prevalence of fks1 hot spot 1 mutations in a worldwide collection of Candida strains. Antimicrob Agents Chemother 54:2655-9.

87. Hori Y, Shibuya K. 2018. Role of FKS Gene in the Susceptibility of Pathogenic Fungi to Echinocandins. Med Mycol J 59:E31-e40.

88. Park S, Kelly R, Kahn JN, Robles J, Hsu MJ, Register E, Li W, Vyas V, Fan H, Abruzzo G, Flattery A, Gill C, Chrebet G, Parent SA, Kurtz M, Teppler H, Douglas CM, Perlin DS. 2005. Specific Substitutions in the Echinocandin Target Fks1p Account for Reduced Susceptibility of Rare Laboratory and Clinical Candida sp. Isolates. Antimicrobial Agents and Chemotherapy 49:3264-3273.

89. Aruanno M, Glampedakis E, Lamoth F. 2019. Echinocandins for the Treatment of Invasive Aspergillosis: from Laboratory to Bedside. Antimicrob Agents Chemother 63.

90. Aguilar-Zapata D, Petraitiene R, Petraitis V. 2015. Echinocandins: The Expanding Antifungal Armamentarium. Clinical Infectious Diseases 61:S604-S611.

91. Arendrup MC, Perkhofer S, Howard SJ, Garcia-Effron G, Vishukumar A, Perlin D, Lass-Flörl C. 2008. Establishing In Vitro-In Vivo Correlations for Aspergillus fumigatus: the Challenge of Azoles versus Echinocandins. Antimicrobial Agents and Chemotherapy 52:3504-3511.

92. e Silva AP, Miranda IM, Branco J, Oliveira P, Faria-Ramos I, Silva RM, Rodrigues AG, Costa-de-Oliveira S. 2020. FKS1 mutation associated with decreased echinocandin susceptibility of Aspergillus fumigatus following anidulafungin exposure. Scientific Reports 10:11976.

93. Fisher MC, Denning DW. 2023. The WHO fungal priority pathogens list as a game-changer. Nature Reviews Microbiology 21:211-212.

94. Anonymous. 2022. WHO fungal priority pathogens list to guide research, development and public health action. World Health Organization, WHO.

95. Roemer T, Krysan DJ. 2014. Antifungal drug development: challenges, unmet clinical needs, and new approaches. Cold Spring Harbor perspectives in medicine 4:a019703.

96. Carolus H, Pierson S, Lagrou K, Van Dijck P. 2020. Amphotericin B and Other Polyenes—Discovery, Clinical Use, Mode of Action and Drug Resistance. Journal of Fungi 6:321.

97. Cowen LE, Sanglard D, Howard SJ, Rogers PD, Perlin DS. 2014. Mechanisms of Antifungal Drug Resistance. Cold Spring Harbor perspectives in medicine 5:a019752-a019752.

98. Walker LA, Munro CA, de Bruijn I, Lenardon MD, McKinnon A, Gow NAR. 2008. Stimulation of Chitin Synthesis Rescues Candida albicans from Echinocandins. PLOS Pathogens 4:e1000040.

99. Harris BE, Manning BW, Federle TW, Diasio RB. 1986. Conversion of 5-fluorocytosine to 5-fluorouracil by human intestinal microflora. Antimicrob Agents Chemother 29:44-8.

100. Chen R, Wong HL, Burns BP. 2019. New Approaches to Detect Biosynthetic Gene Clusters in the Environment. Medicines (Basel, Switzerland) 6:32.

101. Oliver JD, Sibley GEM, Beckmann N, Dobb KS, Slater MJ, McEntee L, du Pré S, Livermore J, Bromley MJ, Wiederhold NP, Hope WW, Kennedy AJ, Law D, Birch M. 2016. F901318 represents a novel class of antifungal drug that inhibits dihydroorotate dehydrogenase. Proc Natl Acad Sci U S A 113:12809-12814.

102. Wiederhold NP. 2020. Review of the Novel Investigational Antifungal Olorofim. Journal of fungi (Basel, Switzerland) 6:122.

103. Ghannoum M, Arendrup MC, Chaturvedi VP, Lockhart SR, McCormick TS, Chaturvedi S, Berkow EL, Juneja D, Tarai B, Azie N, Angulo D, Walsh TJ. 2020. Ibrexafungerp: A Novel Oral Triterpenoid Antifungal in Development for the Treatment of Candida auris Infections. Antibiotics 9:539.

104. Gamal A, Chu S, McCormick TS, Borroto-Esoda K, Angulo D, Ghannoum MA. 2021. Ibrexafungerp, a Novel Oral Triterpenoid Antifungal in Development: Overview of Antifungal Activity Against Candida glabrata. Frontiers in Cellular and Infection Microbiology 11.

105. Hoenigl M, Sprute R, Egger M, Arastehfar A, Cornely OA, Krause R, Lass-Flörl C, Prattes J, Spec A, Thompson GR, Wiederhold N, Jenks JD. 2021. The Antifungal

Pipeline: Fosmanogepix, Ibrexafungerp, Olorofim, Opelconazole, and Rezafungin. Drugs 81:1703-1729.

106. Sekurova ON, Schneider O, Zotchev SB. 2019. Novel bioactive natural products from bacteria via bioprospecting, genome mining and metabolic engineering. Microbial biotechnology 12:828-844.

107. Newman DJ, Cragg GM. 2016. Natural Products as Sources of New Drugs from 1981 to 2014. J Nat Prod 79:629-61.

108. Zhang B, Zhou Y-T, Jiang S-X, Zhang Y-H, Huang K, Liu Z-Q, Zheng Y-G. 2020. Amphotericin B biosynthesis in Streptomyces nodosus: quantitative analysis of metabolism via LC–MS/MS based metabolomics for rational design. Microbial Cell Factories 19:18.

109. Szymański M, Chmielewska S, Czyżewska U, Malinowska M, Tylicki A. 2022. Echinocandins - structure, mechanism of action and use in antifungal therapy. J Enzyme Inhib Med Chem 37:876-894.

110. Eustáquio AS, Ziemert N. Identification of Natural Product Biosynthetic Gene Clusters from Bacterial Genomic Data, p 1-21 doi:10.1007/7653_2018_32. Humana Press, Totowa, NJ.

111. Bredholt H, Fjærvik E, Johnsen G, Zotchev SB. 2008. Actinomycetes from Sediments in the Trondheim Fjord, Norway: Diversity and Biological Activity. Marine Drugs 6:12-24.

112. Zhang F, Zhao M, Braun DR, Ericksen SS, Piotrowski JS, Nelson J, Peng J, Ananiev GE, Chanana S, Barns K, Fossen J, Sanchez H, Chevrette MG, Guzei IA, Zhao C, Guo L, Tang W, Currie CR, Rajski SR, Audhya A, Andes DR, Bugni TS. 2020. A marine microbiome antifungal targets urgent-threat drug-resistant fungi. Science 370:974-978.

113. Zhao M, Zhang F, Zarnowski R, Barns K, Jones R, Fossen J, Sanchez H, Rajski SR, Audhya A, Bugni TS, Andes DR. 2021. Turbinmicin inhibits Candida biofilm growth by disrupting fungal vesicle-mediated trafficking. J Clin Invest 131.

114. Gregory AC, Zayed AA, Conceição-Neto N, Temperton B, Bolduc B, Alberti A, Ardyna M, Arkhipova K, Carmichael M, Cruaud C, Dimier C, Domínguez-Huerta G, Ferland J, Kandels S, Liu Y, Marec C, Pesant S, Picheral M, Pisarev S, Poulain J, Tremblay J-É, Vik D, Acinas SG, Babin M, Bork P, Boss E, Bowler C, Cochrane G, de Vargas C, Follows M, Gorsky G, Grimsley N, Guidi L, Hingamp P, Iudicone D, Jaillon O, Kandels-Lewis S, Karp-Boss L, Karsenti E, Not F, Ogata H, Pesant S, Poulton N, Raes J, Sardet C, Speich S, Stemmann L, Sullivan MB, Sunagawa S, Wincker P, et al. 2019. Marine DNA Viral Macro- and Microdiversity from Pole to Pole. Cell 177:1109-1123.e14.

115. Marcolefas E, Leung T, Okshevsky M, McKay G, Hignett E, Hamel J, Aguirre G, Blenner-Hassett O, Boyle B, Lévesque RC, Nguyen D, Gruenheid S, Whyte L. 2019. Culture-Dependent Bioprospecting of Bacterial Isolates From the Canadian High Arctic Displaying Antibacterial Activity. Frontiers in Microbiology 10.

116. Classen A. 2021. Discovery of novel cold-active antifungals from polar bacteria isolated from the Canadian high arctic that are active against major spoilage fungi in the cheese industry. Masters of Science. McGill University

117. Medema MH, Blin K, Cimermancic P, de Jager V, Zakrzewski P, Fischbach MA, Weber T, Takano E, Breitling R. 2011. antiSMASH: rapid identification, annotation and analysis of secondary metabolite biosynthesis gene clusters in bacterial and fungal genome sequences. Nucleic acids research 39:W339-W346.

118. Kwon-Chung KJ, Sugui JA. 2013. Aspergillus fumigatus--what makes the species a ubiquitous human fungal pathogen? PLoS Pathog 9:e1003743.

119. Bahuguna A, Khan, Imran, Bajpai, Vivek K., Kang, Sun Chul 2017. MTT assay to evaluate the cytotoxic potential of a drug. Bangladesh Journal of Pharmacology 12.

120. CLSI. 2002. Reference Method for Broth Dilution Antifungal Susceptibility Testing of Filamentous Fungi; Approved Standard Clinical and Laboratory Standards Institute, Wayne, PA.

121. Wang M, Carver JJ, Phelan VV, Sanchez LM, Garg N, Peng Y, Nguyen DD, Watrous J, Kapono CA, Luzzatto-Knaan T, Porto C, Bouslimani A, Melnik AV, Meehan MJ, Liu W-T, Crüsemann M, Boudreau PD, Esquenazi E, Sandoval-Calderón M, Kersten RD, Pace LA, Quinn RA, Duncan KR, Hsu C-C, Floros DJ, Gavilan RG, Kleigrewe K, Northen T, Dutton RJ, Parrot D, Carlson EE, Aigle B, Michelsen CF, Jelsbak L, Sohlenkamp C, Pevzner P, Edlund A, McLean J, Piel J, Murphy BT, Gerwick L, Liaw C-C, Yang Y-L, Humpf H-U, Maansson M, Keyzers RA, Sims AC, Johnson AR, Sidebottom AM, Sedio BE, et al. 2016. Sharing and community curation of mass spectrometry data with Global Natural Products Social Molecular Networking. Nature Biotechnology 34:828-837.

122. Ostapska H, Raju D, Lehoux M, Lacdao I, Gilbert S, Sivarajah P, Bamford Natalie C, Baker P, Nguyen Thi Tuyet M, Zacharias Caitlin A, Gravelat Fabrice N, Howell PL, Sheppard Donald C. 2021. Preclinical Evaluation of Recombinant Microbial Glycoside Hydrolases in the Prevention of Experimental Invasive Aspergillosis. mBio 12:10.1128/mbio.02446-21.

123. Stewart James IP, Fava Vinicius M, Kerkaert Joshua D, Subramanian Adithya S, Gravelat Fabrice N, Lehoux M, Howell PL, Cramer Robert A, Sheppard Donald C. 2020.

Reducing Aspergillus fumigatus Virulence through Targeted Dysregulation of the Conidiation Pathway. mBio 11:10.1128/mbio.03202-19.

124. Bankhead P, Loughrey MB, Fernández JA, Dombrowski Y, McArt DG, Dunne PD, McQuaid S, Gray RT, Murray LJ, Coleman HG, James JA, Salto-Tellez M, Hamilton PW. 2017. QuPath: Open source software for digital pathology image analysis. Scientific Reports 7:16878.

125. Inc. TFS. 2009. Acetone precipitation of proteins

126. Searle BC. 2010. Scaffold: a bioinformatic tool for validating MS/MS-based proteomic studies. Proteomics 10:1265-9.

127. Basenko EY, Pulman JA, Shanmugasundram A, Harb OS, Crouch K, Starns D, Warrenfeltz S, Aurrecoechea C, Stoeckert CJ, Jr., Kissinger JC, Roos DS, Hertz-Fowler C. 2018. FungiDB: An Integrated Bioinformatic Resource for Fungi and Oomycetes. J Fungi (Basel) 4.

128. Priebe S, Kreisel C, Horn F, Guthke R, Linde J. 2015. FungiFun2: a comprehensive online resource for systematic analysis of gene lists from fungal species. Bioinformatics 31:445-6.

129. Millette P-G, Chabot J, Sheppard DC, Le Mauff F. 2023. Identification and Quantification of Monosaccharides from Fungal Cell Walls and Exopolysaccharides by Gas Chromatography Coupled to Mass Spectrometry. Current Protocols 3:e853.

130. Kiho T, Nagai K, Ukai S, Haga M. 1992. Structure and antitumor activity of a branched (1→ 3)-β-d-glucan from the alkaline extract of Amanita muscaria. Carbohydrate research 224:237-243.

131. KIHO T, YOSHIDA I, KATSURAGAWA M, SAKUSHIMA M, USUI S, UKAI S. 1994. Polysaccharides in fungi. XXXIV. A polysaccharide from the fruiting bodies of Amanita muscaria and the antitumor activity of its carboxymethylated product. Biological and Pharmaceutical Bulletin 17:1460-1462.

132. Anonymous. 2021. Glucatell® (1,3)-Beta-D-Glucan Detection Reagent Kit vol 9. Associates of Cape Cod Incorporated, Online.

133. Omura S, Iwai Y, Hirano A, Nakagawa A, Awaya J, Tsuchya H, Takahashi Y, Masuma R. 1977. A new alkaloid AM-2282 OF Streptomyces origin. Taxonomy, fermentation, isolation and preliminary characterization. J Antibiot (Tokyo) 30:275-82.

134. Ōmura S, Asami Y, Crump A. 2018. Staurosporine: new lease of life for parent compound of today's novel and highly successful anti-cancer drugs. The Journal of Antibiotics 71:688-701.

135. Steff A-M, Fortin M, Arguin C, Hugo P. 2001. Detection of a decrease in green fluorescent protein fluorescence for the monitoring of cell death: An assay amenable to high-throughput screening technologies. Cytometry 45:237-243.

136. Stepczynska A, Lauber K, Engels IH, Janssen O, Kabelitz D, Wesselborg S, Schulze-Osthoff K. 2001. Staurosporine and conventional anticancer drugs induce overlapping, yet distinct pathways of apoptosis and caspase activation. Oncogene 20:1193-1202.

137. Ullal AJ, Pisetsky DS. 2010. The release of microparticles by Jurkat leukemia T cells treated with staurosporine and related kinase inhibitors to induce apoptosis. Apoptosis 15:586-96.

138. Dunai ZA, Imre G, Barna G, Korcsmaros T, Petak I, Bauer PI, Mihalik R. 2012. Staurosporine induces necroptotic cell death under caspase-compromised conditions in U937 cells. PLoS One 7:e41945.

139. Gani OA, Engh RA. 2010. Protein kinase inhibition of clinically important staurosporine analogues. Nat Prod Rep 27:489-98.

140. Gescher A. 1998. Analogs of staurosporine: potential anticancer drugs? Gen Pharmacol 31:721-8.

141. Mukthavaram R, Jiang P, Saklecha R, Simberg D, Bharati IS, Nomura N, Chao Y, Pastorino S, Pingle SC, Fogal V, Wrasidlo W, Makale M, Kesari S. 2013. High-efficiency liposomal encapsulation of a tyrosine kinase inhibitor leads to improved in vivo toxicity and tumor response profile. Int J Nanomedicine 8:3991-4006.

142. Committee WSUIACaU. 2022. Preparation of Dimethyl Sulfoxide (DMSO) Procedure #1, p 2. Washington State University, Online.

143. Jiang C, Wang H, Liu M, Wang L, Yang R, Wang P, Lu Z, Zhou Y, Zheng Z, Zhao G. 2022. Identification of chitin synthase activator in Aspergillus niger and its application in citric acid fermentation. Appl Microbiol Biotechnol 106:6993-7011.

144. Hu X, Yang P, Chai C, Liu J, Sun H, Wu Y, Zhang M, Zhang M, Liu X, Yu H. 2023. Structural and mechanistic insights into fungal β-1,3-glucan synthase FKS1. Nature 616:190-198.

145. Satish S, Perlin DS. 2019. Echinocandin Resistance in Aspergillus fumigatus Has Broad Implications for Membrane Lipid Perturbations That Influence Drug-Target Interactions. Microbiol Insights 12:1178636119897034.

146. Valiante V, Macheleidt J, Föge M, Brakhage AA. 2015. The Aspergillus fumigatus cell wall integrity signaling pathway: drug target, compensatory pathways, and virulence. Frontiers in Microbiology 6.

147. Kalem MC, Subbiah H, Leipheimer J, Glazier VE, Panepinto JC. 2021. Puf4 Mediates Post-transcriptional Regulation of Cell Wall Biosynthesis and Caspofungin Resistance in Cryptococcus neoformans. mBio 12.

148. Sheppard D. 2020. Development of New Therapeutics Targeting Biofilm Formation by the

Opportunistic Pulmonary Pathogens Pseudomonas aeruginosa and Aspergillus

fumigatus. U.S. Army Medical Research and Materiel Command Defense Technical Information Center.

149. LaFayette SL, Collins C, Zaas AK, Schell WA, Betancourt-Quiroz M, Gunatilaka AAL, Perfect JR, Cowen LE. 2010. PKC Signaling Regulates Drug Resistance of the Fungal Pathogen Candida albicans via Circuitry Comprised of Mkc1, Calcineurin, and Hsp90. PLOS Pathogens 6:e1001069.

150. Xie JL, O'Meara TR, Polvi EJ, Robbins N, Cowen LE. 2017. Staurosporine Induces Filamentation in the Human Fungal Pathogen Candida albicans via Signaling through Cyr1 and Protein Kinase A. mSphere 2:e00056-17.

151. Tamaoki T, Nomoto H, Takahashi I, Kato Y, Morimoto M, Tomita F. 1986. Staurosporine, a potent inhibitor of phospholipidCa++dependent protein kinase. Biochemical and Biophysical Research Communications 135:397-402.

152. Yoshida S, Ikeda E, Uno I, Mitsuzawa H. 1992. Characterization of a staurosporine- and temperature-sensitive mutant, stt1, of Saccharomyces cerevisiae: STT1 is allelic to PKC1. Molecular and General Genetics MGG 231:337-344.

153. Yoshida S, Anraku Y. 2000. Characterization of staurosporine-sensitive mutants of Saccharomyces cerevisiae: vacuolar functions affect staurosporine sensitivity. Molecular and General Genetics MGG 263:877-888.

154. Jin J, Iwama R, Horiuchi H. 2023. The N-terminal disordered region of ChsB regulates its efficient transport to the hyphal apical surface in Aspergillus nidulans. Current Genetics 69:175-188.

155. Schaefer AL, Ceesay M, Leier JA, Tesch J, Wisenden BD, Pandey S. 2020. Factors Contributing to Sex Differences in Mice Inhaling Aspergillus fumigatus. Int J Environ Res Public Health 17.

156. Chuan L, Zhang J, Yu-Jiao Z, Shu-Fang N, Jun C, Qian W, Shao-Ping N, Ze-Yuan D, Ming-Yong X, Shu W. 2015. Biocompatible and biodegradable nanoparticles for enhancement of anti-cancer activities of phytochemicals. Chinese journal of natural medicines 13:641-652.

157. Hamill RJ. 2013. Amphotericin B Formulations: A Comparative Review of Efficacy and Toxicity. Drugs 73:919-934.

158. Meagher RB, Lewis ZA, Ambati S, Lin X. 2021. Aiming for a bull's-eye: Targeting antifungals to fungi with dectin-decorated liposomes. PLOS Pathogens 17:e1009699.

159. Ambati S, Ferarro AR, Kang SE, Lin J, Lin X, Momany M, Lewis ZA, Meagher RB. 2019. Dectin-1-Targeted Antifungal Liposomes Exhibit Enhanced Efficacy. mSphere 4.

160. Ambati S, Pham T, Lewis ZA, Lin X, Meagher RB. 2022. DectiSomes: Glycan Targeting of Liposomal Drugs Improves the Treatment of Disseminated Candidiasis. Antimicrob Agents Chemother 66:e0146721.

161. Perez-Cuesta U, Guruceaga X, Cendon-Sanchez S, Pelegri-Martinez E, Hernando FL, Ramirez-Garcia A, Abad-Diaz-de-Cerio A, Rementeria A. 2021. Nitrogen, Iron and Zinc Acquisition: Key Nutrients to Aspergillus fumigatus Virulence. J Fungi (Basel) 7.

162. Akhtar N, Karabika E, Kinghorn JR, Glass ADM, Unkles SE, Rouch DA. 2015. High-affinity nitrate/nitrite transporters NrtA and NrtB of Aspergillus nidulans exhibit high specificity and different inhibitor sensitivity. Microbiology 161:1435-1446.

163. Deshmukh M, Johnson EM, Jr. 2000. Staurosporine-induced neuronal death: multiple mechanisms and methodological implications. Cell Death Differ 7:250-61.

164. Belmokhtar CA, Hillion J, Ségal-Bendirdjian E. 2001. Staurosporine induces apoptosis through both caspase-dependent and caspase-independent mechanisms. Oncogene 20:3354-62.

165. Circu ML, Stringer S, Rhoads CA, Moyer MP, Aw TY. 2009. The role of GSH efflux in staurosporine-induced apoptosis in colonic epithelial cells. Biochem Pharmacol 77:76-85.

166. Nierman WC, Pain A, Anderson MJ, Wortman JR, Kim HS, Arroyo J, Berriman M, Abe K, Archer DB, Bermejo C, Bennett J, Bowyer P, Chen D, Collins M, Coulsen R, Davies R, Dyer PS, Farman M, Fedorova N, Fedorova N, Feldblyum TV, Fischer R, Fosker N, Fraser A, García JL, García MJ, Goble A, Goldman GH, Gomi K, Griffith-Jones S, Gwilliam R, Haas B, Haas H, Harris D, Horiuchi H, Huang J, Humphray S, Jiménez J, Keller N, Khouri H, Kitamoto K, Kobayashi T, Konzack S, Kulkarni R, Kumagai T, Lafton A, Latgé J-P, Li W, Lord A, Lu C, et al. 2005. Genomic sequence of the

pathogenic and allergenic filamentous fungus Aspergillus fumigatus. Nature 438:1151-1156.

167. Fernandes AS, Gonçalves AP, Castro A, Lopes TA, Gardner R, Glass NL, Videira A. 2011. Modulation of fungal sensitivity to staurosporine by targeting proteins identified by transcriptional profiling. Fungal Genet Biol 48:1130-8.

168. Satish S, Jiménez-Ortigosa C, Zhao Y, Lee MH, Dolgov E, Krüger T, Park S, Denning DW, Kniemeyer O, Brakhage AA, Perlin DS. 2019. Stress-Induced Changes in the Lipid Microenvironment of β-(1,3)-d-Glucan Synthase Cause Clinically Important Echinocandin Resistance in Aspergillus fumigatus. mBio 10:e00779-19.

169. Ibrahim AS, Spellberg B, Walsh TJ, Kontoyiannis DP. 2012. Pathogenesis of mucormycosis. Clinical infectious diseases : an official publication of the Infectious Diseases Society of America 54 Suppl 1:S16-S22.

170. Chater KF. 2006. Streptomyces inside-out: a new perspective on the bacteria that provide us with antibiotics. Philos Trans R Soc Lond B Biol Sci 361:761-8.

171. Alam K, Abbasi MN, Hao J, Zhang Y, Li A. 2021. Strategies for Natural Products Discovery from Uncultured Microorganisms. Molecules 26.